Secondary Natural Gas Recovery:

Use of Dipmeters in Stratigraphic and Depositional Interpretation of Natural Gas Reservoirs of the Oligocene Vicksburg Formation: An Example from McAllen Ranch Field, Hidalgo County Texas, of Targeted Technology Applications for Infield Reserve Growth.

Topical Report

Oct. 1989 - Feb. 1992

Prepared by:

R. P. Langford

Bureau of Economic Geology,
W. L. Fisher, Director
The University of Texas at Austin
Austin, Texas   78713-7508

J. D. Hall

ResTech Houston, Inc.
Houston, Texas

February 1992

QAe7659

GRI DISCLAIMER

REPORT DOCUMENTATION PAGE	1. REPORT NO. 50272-101	2.	3. Recipient's Accession No.		
4. Title and Subtitle Secondary Natural Gas Recovery: Use of Dipmeters in Stratigraphic and Depositional Interpretation of Natural Gas Reservoirs of the Oligocene Vicksburg Formation: An Example from McAllen Ranch Field, Hidalgo County Texas of Targeted Technology Applications for Infield Reserve Growth.			5. Report Date January 1992		
			6.		
7. Author(s) R. P. Langford & J. D. Hall			8. Performing Organization Rept. No.		
9. Performing Organization ResTech Houston, Inc. 3707 FM 1960 West, Suite 400 Houston, Texas 77068-3555			10. Project/Task/Work Unit No.		
			11. Contract(C) or Grant(G) No. (C) GRI NO. 5088-212-1718 (G)DOE NO. DE-FG21-88MC25031		
12. Sponsoring Organization Name and Address Gas Research Institute 8600 West Bryn Mawr Avenue Chicago, Illinois 60631			13. Type of Report & Period Covered Topical Report Oct. 1989 - Feb. 1991		
			14.		

15. Supplementary Notes

16. Abstract (Limit: 200 words)

Dipmeter interpretation techniques based on the correlation of dipmeter results with maps, cores, and VSP have been developed to aid in the identification of secondary gas recovery in the Vicksburg section of McAllen Ranch Field in South Texas. The objectives of this program include the identification of optimal dipmeter processing parameters to match structural and stratigraphic features in the cores; integration of structural dipmeter results into the structural mapping; correlation of dipmeter results to depositional dips in the cores to identify interpretation methods for predicting sand developments between well bores; and identification of growth fault associated structural features that tend to cause reservoir compartments.

Results of these efforts have been documented and the dipmeter results aided in the description of the reservoir. Dipmeter processing parameters were identified that produced results reflecting structural and stratigraphic features in the cores. Large slump features interpreted from the dipmeter were interpreted from the VSP. Numerous small slump features indicate the orientation of permeability reductions. Microresistivity curves were correlated with cement types in the core allowing qualitative permeability predictions. Hole breakouts were compared to acoustic anisotropy to predict formation stress vectors.

17. Document Analysis   a. Descriptors
Gas Fields
Vicksburg
Growth Faults
Mapping

b. Identifiers/Open-Ended Terms
Well Log Interpretation
Geology
Earth Sciences
Petrology
Seismic

c. COSATI Field/Group

18. Availability Statement	19. Security Class (This Report) Unclassified	21. No. of Pages 93
	20. Security Class (This Page)	22. Price

RESEARCH SUMMARY

Title:
Secondary Natural Gas Recovery: Use of Dipmeters in Stratigraphic and Depositional Interpretation of Natural Gas Reservoirs of the Oligocene Vicksburg Formation: An Example from McAllen Ranch Field, Hidalgo County Texas of Targeted Technology Applications for Infield Reserve Growth.

Contractor:
The Bureau of Economic Geology
The University of Texas at Austin
GRI Contract No. 5088-212-1718
DOE Contract No. DE-FG21-88MC25031

Subcontractor:
ResTech Houston, Inc.
Houston, Texas

Principal
Investigators:
R. J. Finley and R. A. Levey
Bureau of Economic Geology
The University of Texas at Austin

Project
Managers:
W. E. Howard and J. D. Hall
ResTech Houston, Inc.

Report Period:
Topical Report, October 1989 - February 1992

Objectives:
To improve the analysis and interpretation of dipmeters in growth faulted environments, identify methods for integration into mapping and seismic interpretation, identify methods of using the dipmeter to interpret sedimentary features observed in cores and orient hole breakouts to formation stress data and to apply these techniques to the search for incremental reserves in mature natural gas fields.

Technical
Perspective:
The Gas Research Institute (GRI) has been conducting research directed at identifying methods of detecting and tapping incremental natural gas in existing fields. The dipmeter provides measurements that can be extrapolated away from the wellbore and aid in the integration of well data into field wide data such as well-to-well correlations and seismic data. The McAllen Ranch field provided a base of dipmeter data in a growth fault-dominated mature Vicksburg gas field where new wells are being drilled.

Optimum application of the dipmeter involves data acquisition, processing, display and interpretation. Processing parameters were optimized by comparing various computed results to the sedimentary features observed in cores. Critical structural

and sedimentary anomalies can be identified on the dipmeter. Structural and sedimentary results from the dipmeter can then be extrapolated to other zones and wells that were not cored. The interpretation of these results can be integrated with mapping, production, and seismic data.

The dipmeter 4-arm calipers can be processed for hole breakout orientation and compared to formation stress data for planning hydraulic fracture treatments.

Technical
Approach:

Dipmeters and other logs from 15 wells from the Shell McAllen "B" lease in Hidalgo County, Texas were entered into a database maintained for the Gas Research Institute. All wells were processed for structural dip data, and five wells, including two with cores, were processed for stratigraphic dip data. Processing parameters were optimized to give the best results compared to cores. Expanded scale microresistivity curves were compared to cores to determine the type and scale of features that could be identified. Processing parameters were adjusted to enhance the dipmeter results compared to the features.

Dipmeter results and other logs were plotted on various depth scales from 1:1 to 1:5000 to provide correlations to data from the scale of cores to seismic. Schmidt plots were made of the various sandstones and apparent structural anomalies to detect any change in azimuth in the vertical section and between wells. Dip projections were made along VSP and seismic lines and between wells.

Calipers were processed to identify the degree and azimuth of hole elongation through the S zone. These results were compared to acoustic anisotropy data from cores.

All data were added to the Secondary Gas Recovery project data base.

Results:

Rotation of strata into a major growth fault WNW of the Shell McAllen Ranch B area is the predominant influence on all dipmeters. The sediments affected by the growth fault can be divided into stratigraphically defined domains, rotated to approximately the same dips and azimuths. The variation in azimuths of rotation indicates that the area of maximum subsidence shifted along the fault. Since in a growth fault zone, the area of maximum subsidence corresponds to the area of maximum deposition and thus the thickest reservoir sandstones, the inferences drawn from the azimuths of rotation can be used to infer the direction of offset sandstone thicks. This technique successfully predicts the thickness patterns within the S_1 and S_2 sandstones of the Vicksburg S reservoir.

Wells with axes of rotation that vary from the rest may be inferred to be separated by active growth faults. This technique successfully predicted a growth fault that was subsequently imaged on three-dimensional seismic between the B-3 well and the rest of the B area wells.

Changes in the number and character of dip domains within the growth fault-influenced section may be used to infer that intervals are not stratigraphically correlative. This technique allows correct interpretation of stratigraphic change rather than fault offset of the S reservoir along the western margin of the B area. A similar reinterpretation by Shell Western E & P resulted in 100 Bcf of added reserves since 1987 (Hill and others, 1991).

Slumps provide a potential source of reservoir heterogeneity that must be considered in fields with similar depositional environments. Numerous slumps and small faults pervade the stratigraphic interval affected by the growth fault. These

slumps are down toward the fault and are interpreted to reduce the permeability in the direction of the fault. A large slump was also evident on the VSP. Interpretation of these slumps aided in the geologic interpretation of the movement of the growth fault and associated deltaic sequences.

Hole breakout azimuths on five wells were compared to azimuths derived from acoustic anisotropy to define formation stress vectors. The two measurement techniques agreed within 23°. This is considered a good match because of the low precision of acoustical anisotropy results. This comparison indicates that hole eccentricity can be used to predict horizontal stress vectors. These results proved extremely useful in creating a reservoir model of part of the S reservoir in the B area that was used to quantify permeability barriers within the area and to identify areas with potential for unrecovered resources.

Project Implications:

This report summarizes the results of dipmeter analysis performed as part of a broader project to investigate targeted technology applications for infield reserve growth. Analysis of dipmeter logs for both stratigraphic and structural relationships can be used to verify the position of faults, determine depositional environment of the reservoir, and identify internal reservoir heterogeneity such as syndepositional slumping which could affect gas flow within reservoirs. In addition, dipmeter analysis can be used to predict sandstone thicks within gas bearing intervals for targeting infield completions. Dipmeter data have supported a geological and seismically compatible reinterpretation that eliminated an inferred fault boundary of the major S-reservoir package within McAllen Ranch field. Similar combined geologic-petrophysical studies could result in significant reserve additions by operators in other Vicksburg producing gas fields.

TABLE OF CONTENTS

LIST OF FIGURES

LIST OF TABLES

INTRODUCTION

OBJECTIVES

This report summarizes a study of dipmeter logs from 15 wells within the S reservoir in the B area of McAllen Ranch field in northern Hidalgo County, Texas. The study is part of a research effort funded by the Gas Research Institute, the U.S. Department of Energy, and the State of Texas to identify untapped and poorly drained reservoir compartments by determining the nature of heterogeneity within natural gas reservoirs. Dipmeter data were used in conjunction with stratigraphy interpreted from well logs and vertical seismic profiles to determine and map potential faults and to help in determining reservoir continuity and depositional environment (Langford and others, in press).

The most commonly described reserve additions in lower Vicksburg natural gas fields similar to McAllen Ranch result from reservoir extensions due to reinterpretation of reservoir structure and stratigraphy within the fields (Gardner, 1967; Ashford, 1972; Richards, 1986; Hill and others, 1991). Due to the extreme structural and stratigraphic changes between wells within lower Vicksburg reservoirs, structural and stratigraphic interpretations are difficult. This report describes dipmeter data from one reservoir in McAllen Ranch field where previous correlation of well logs and seismic data had resulted in an interpretation that the S reservoir was cut out by faults in several places. Shell Western E & P has booked over 100 Bcf of added reserves through a reinterpretation that eliminated the inferred faults and allowed drilling of 18 new productive infield wells that expanded the known productive limits of the Vicksburg S reservoir within the confines of McAllen Ranch field since 1987 (Hill and others, 1991).

This report illustrates how dipmeters may be analyzed to improve understanding of the stratigraphic and structural relationships within Vicksburg reservoirs. Similar analysis may lead to definition of reserve growth potential in natural gas reservoirs similar to the S reservoir in McAllen Ranch

1

field. The report demonstrates how dipmeters may be used to predict sandstone thicks within the reservoir in offset locations. These results are important in defining reservoirs with recovery potential, and in locating infield wells and recompletions to recover these resources. The report also describes a method for determining the azimuth direction of hydraulic fractures. This method was useful in modeling part of the Vicksburg S reservoir and in mapping potential unrecovered resources within the B area. Dipmeter interpretations and methodologies reported here were developed by J. Hall of ResTech, Houston and geologic and core correlations are by R. Langford, Bureau of Economic Geology, University of Texas at Austin.

BACKGROUND

The dipmeter logs were recorded from the Vicksburg Formation of South Texas, a lower Oligocene sandstone and shale sequence that forms part of the Gulf Basin fill (fig. 1). McAllen Ranch field is located approximately 20 mi (30 km) down dip of the Vicksburg Fault Zone, on the downthrown, east block of a major growth fault (fig. 2). The Vicksburg Formation expands from 5,000 ft (1,520 m) in thickness on the upthrown block to a maximum of 8,000 ft (2,440 m) within McAllen Ranch field (Marshall, 1981). The strata dip westward into the fault and generally form a shingled set of reservoirs that are progressively younger to the west.

The Vicksburg Formation at McAllen Ranch field is divisible into a shaly upper part and a sandy lower interval (fig. 1) (Marshall, 1978; Shoemaker, 1978; Han, 1981). The sandy lower Vicksburg is interpreted as deposits of fault-localized shelf-edge deltas (Ritch and Kozik, 1971; Picou, 1981). The shaly upper part was deposited as offshore muds. A series of sandstone reservoirs is labeled from youngest to oldest, J through Y (fig. 3). The most volumetrically important gas reservoirs are the Vicksburg P, R, S, and UV. The reservoirs are similar in their internal stratigraphy, consisting of one or more upward-coarsening 30 to 500 ft (10 to 150 m) thick sandstone intervals. The B area lies in the northwestern corner of the field (fig. 2). At the time this study was conducted, 14 wells were drilled into
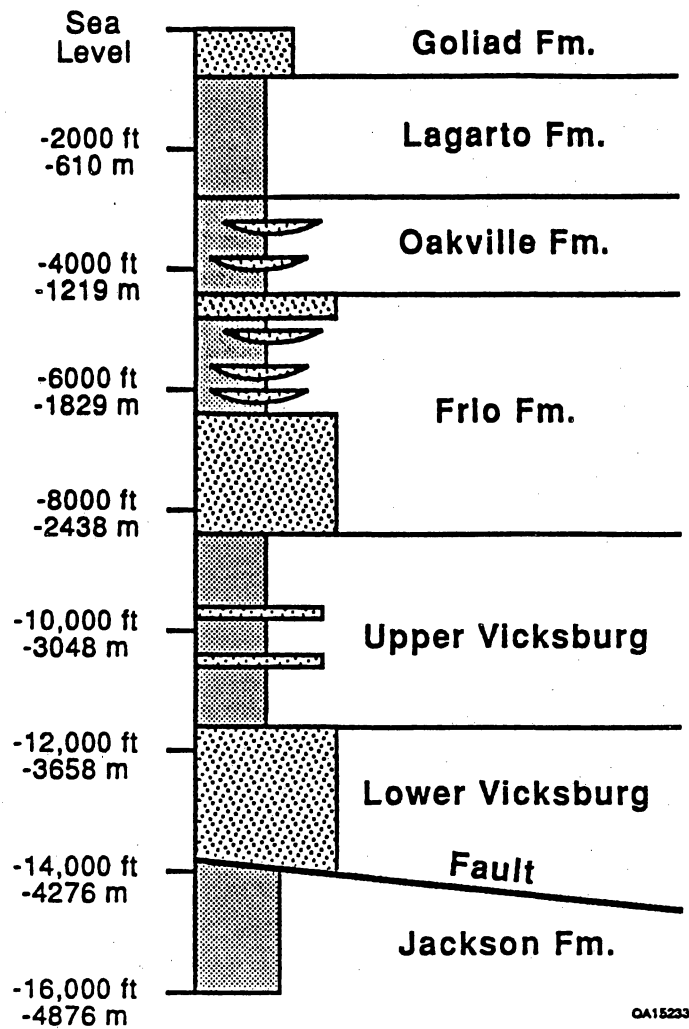
Figure 1. Stratigraphic nomenclature of McAllen Ranch area.
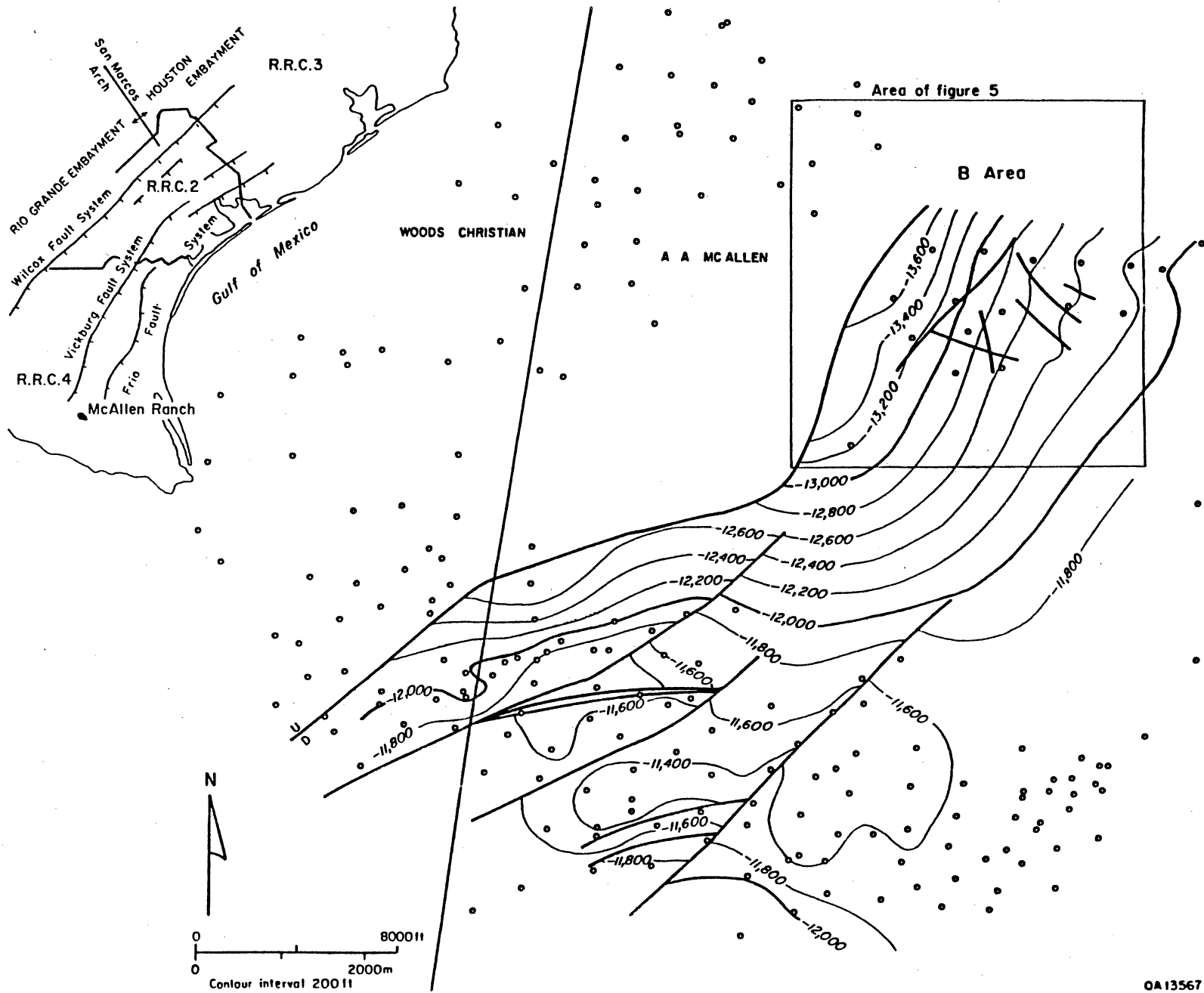
Figure 2. Structure contour map of top of the S reservoir. A greater density of faults is known in the B area due to high-quality, 3-D seismic data, which allow delineation of faults with small throws. In fact, the B area is much less faulted than the rest of the S reservoir producing area. Inset: Map of the South Texas Gulf Coastal Plain showing the location of McAllen Ranch field and the main tectonic features in the area.

TYPE LOG MCALLEN

Frio   7500

Top L. Vicksburg

Vicksburg
L

Vicksburg
J

Vicksburg
M

Vicksburg
K

Vicksburg
N /

Vicksburg
P
/

Vicksburg
R

Vicksburg
S

12,000

SP Res
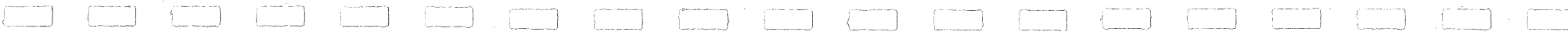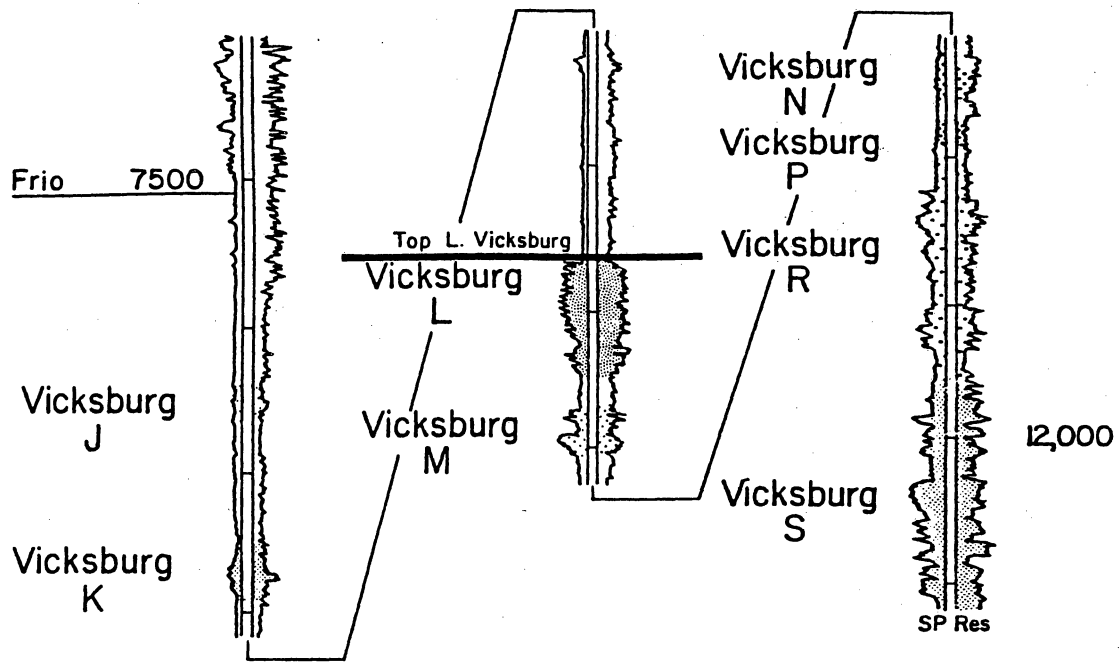
QA11977

Figure3. Type log (A. A. McAllen B-14 well) illustrating the stratigraphy of the Vicksburg reservoirs at McAllen Ranch field.

5

the S reservoir within the B area (fig. 4). However, additional step-out wells were being drilled during the preparation of this report.

A prominent flat-lying detachment fault underlies the field. This fault intersects and cuts the top of the S reservoir just west of the B area (fig. 2). Several minor faults having no obvious trend are visible on seismic data within the B area (fig. 2).

In the B area, the S is the predominant gas reservoir. It ranges in thickness from 1,150 ft (350.5 m) in well B-3 to 300 ft (91.4 m) in wells B-11 and B-14. The reservoir forms a convex-upward, eastward-tapering wedge. The wedge dips toward the faults, with dips at the top of the S ranging from 6° in wells B-11 and B-14, and 12° in wells B-1, B-7, and 7° in well B-3. The reservoir consists of six stacked progradational sandstone intervals deposited by a shelf-margin delta. These intervals are termed the S_1 through S_6 sandstones (fig. 5). Deposition coincided with deformation on the underlying fault, and the sandstones rapidly shale out to the north and east. The S_2 and S_4 are the only two sandstones that extend eastward of well B-11. Diagenesis is an important factor in the productivity of the reservoir (Langford and Lynch, 1990).
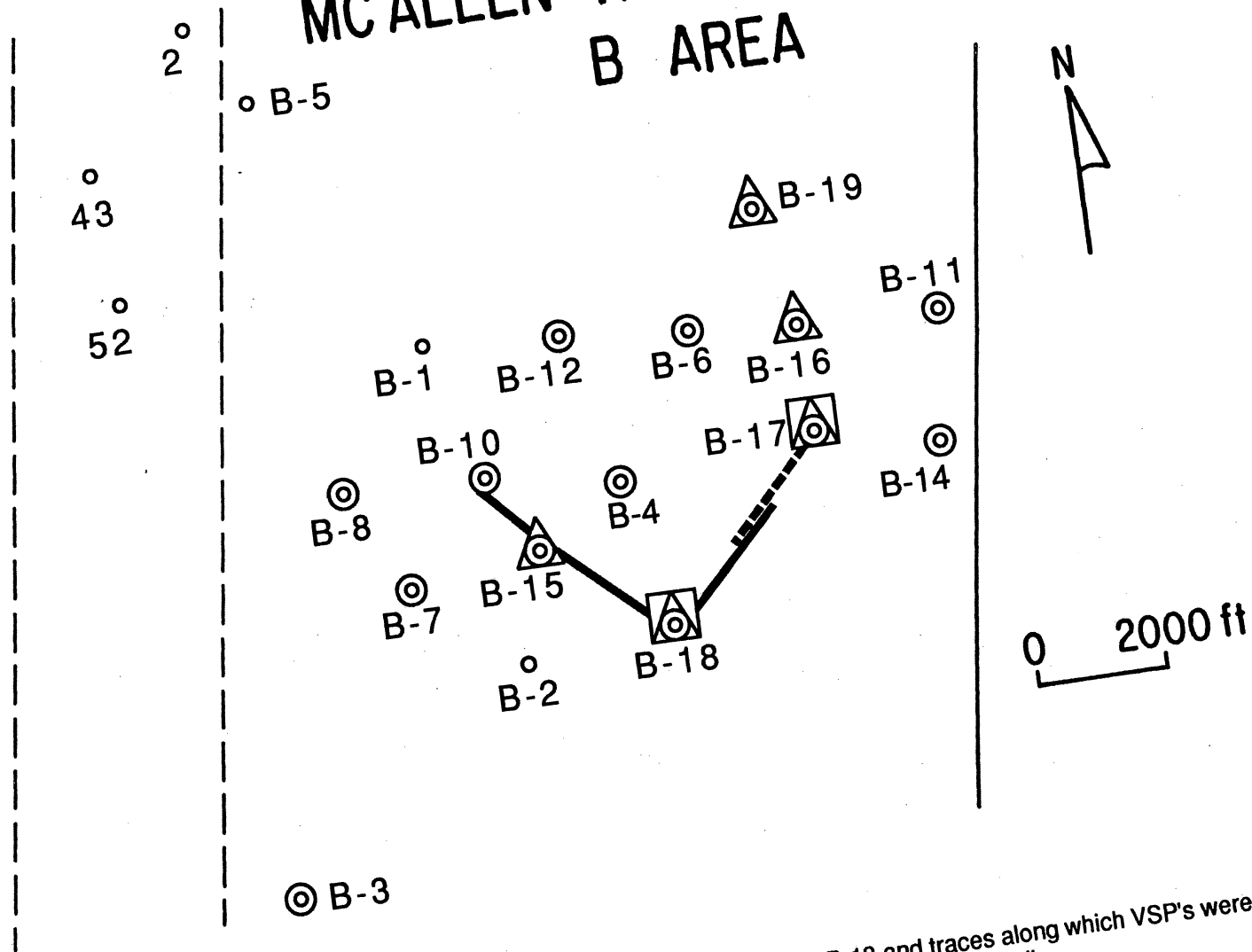
Figure 4. Map of B lease of McAllen Ranch field showing locations of wells B-17 and B-18 and traces along which VSP's were shot. Circle indicates dipmeter log available. Triangle indicates acquisition data available. Square indicates cored wells.
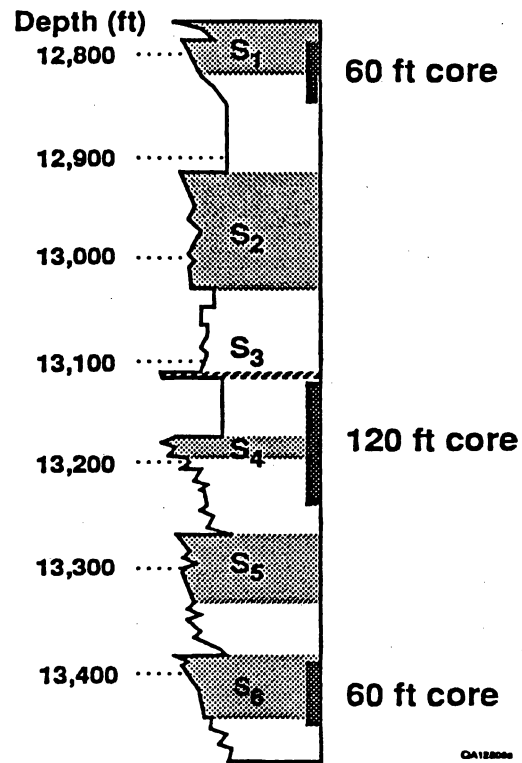
Figure 5. Stratigraphic section through Shell A. A. McAllen B-18 well showing S_1 -S_6 sandstone intervals and location of cores taken for this project.

DATABASE AND METHODOLOGY

INTRODUCTION

The dipmeter data used in this study have been integrated with other logging and core data from McAllen Ranch (Langford and others, 1990) into a unique data set for the interpretation of formation dips in conjunction with other formation information. These data are summarized in table 1. Data on 10 wells contained graphical plots of computed formation dips only. Original acquisition data were available from an additional 5 wells. The data from these 5 wells were reprocessed by ResTech using multiple computation parameters selected to emphasize both structural and stratigraphic information.

DATA TYPES AND EDITING PROCEDURES

The dipmeter data sets contain acquisition data and processed data. The acquisition data were acquired by a logging service company to provide information necessary for computation of the formation dip magnitude and azimuth. These data are broadly classified by logging service companies as "fast channel" and "slow channel" and are recorded at the well on magnetic tape. An analog film is also recorded to verify the validity of the tape data.

Fast-channel refers to the microresistivity curves, which are recorded with pad-mounted electrodes, and to the accelerometer data, which are necessary to correct the curves for variations in tool velocity occurring during the survey. These data are recorded at high sample rates to allow for resolution of the "fast" changing data. The recording rate is of the order of 60 to 120 samples per electrode per foot of well bore. Depending on the particular hardware used, the number of electrodes sampled simultaneously can vary from a minimum of 3 to the current standard of a maximum of 64. The devices used in this study used either 5 or 10 electrodes.

9

Table 1. Wells available with dipmeters.

Well Name*	Dipmeter Interval (ft)	Core Data	Dipmeter Data	Mud System
B-3	10,900-15,100	NO	(1)	Water Base
B-4	11,100-14,915	NO	(1)	Water Base
B-6	11,300-13,850	NO	(1)	Water Base
B-7	10,700-14,100	NO	(1)	Water Base
B-8	11,500-15,000	NO	(1)	Water Base
B-10	10,700-13,800	NO	(1)	Water Base
B-11	10,600-13,740	NO	(1)	Water Base
B-12	11,100-14,440	NO	(1)	Water Base
B-14	11,300-13,830	NO	(1)	Water Base
B-15	9,490-14,650	NO	(2)	Oil Base
B-16	9,048-14,992	NO	(2)	Oil Base
B-17	9,146-14,284	YES	(2)	Oil Base
B-18	9,695-13,963	YES	(2)	Oil Base
B-19	9,775-14,070	NO	(2)	Oil Base

*All wells were operated by Shell Oil Company in the McAllen Ranch Field located in Hidalgo County, Texas.

(1)   Original data acquisition tape not available. Standard logging service company processing results available.   ·

(2)   Original data acquisition tape available. Original and ResTech results available.

Slow-channel refers to data that changes at a "slow" rate and can therefore be sampled at a lower rate. These data are routinely sampled between 2 and 12 times per foot of well bore, including the caliper or calipers, the tool navigation data, and a gamma-ray or SP curve for correlation. Tool navigation data are made up of measurements required to orient the tool in the earth's magnetic and gravitational fields and which can be processed to provide hole directional data and oriented caliper data. The correlation curve is an aid in making depth adjustments to the other depth-based data, such as cores or other logs.

During the several years that the wells studied were drilled, drilling practices evolved from water-based to oil-based muds. The oil-based muds require that dipmeter tools be fitted with "scratcher" electrodes so that the pads can make electrical contact with the rock. This technique can reduce the quality of data by a factor of 90%. However, on the five wells where scratcher electrodes were used (B-15, B-16, B-17, B-18, and B-19) the data quality was very close to that obtained in water-based muds. Figure 6 shows a comparison of computed dips in water-based muds with those in oil-based muds. The water base results are from a four-electrode device, and the oil base results are from an eight-electrode device.

The primary computation made on the raw dipmeter data is the correlation of adjacent resistivity curves. Because of the difficulty in obtaining consistent correlation, resistivity curves are averaged over a correlation length. The interval to be averaged is shifted by a correlation step between each measurement. The computation parameters for the water-based mud are a 4 ft (1.2 m) correlation length, a 2 ft (.6 m) step between correlations, and a 40° search angle (4 ft X 2 ft X 40°). The computation parameters for the oil-based mud are an 8 ft (2.4 m) correlation length, a 2 ft (.6 m) step between correlations, and a 60° search angle (8 ft X 2 ft X 60°). The computation parameters were adjusted so that the oil base dipmeters would yield comparable results to the earlier water base dipmeters. Note that the oil base processing yields have a marginally greater number of scattered points, resulting from noise and poor correlations, but that the overall results are similar.

11
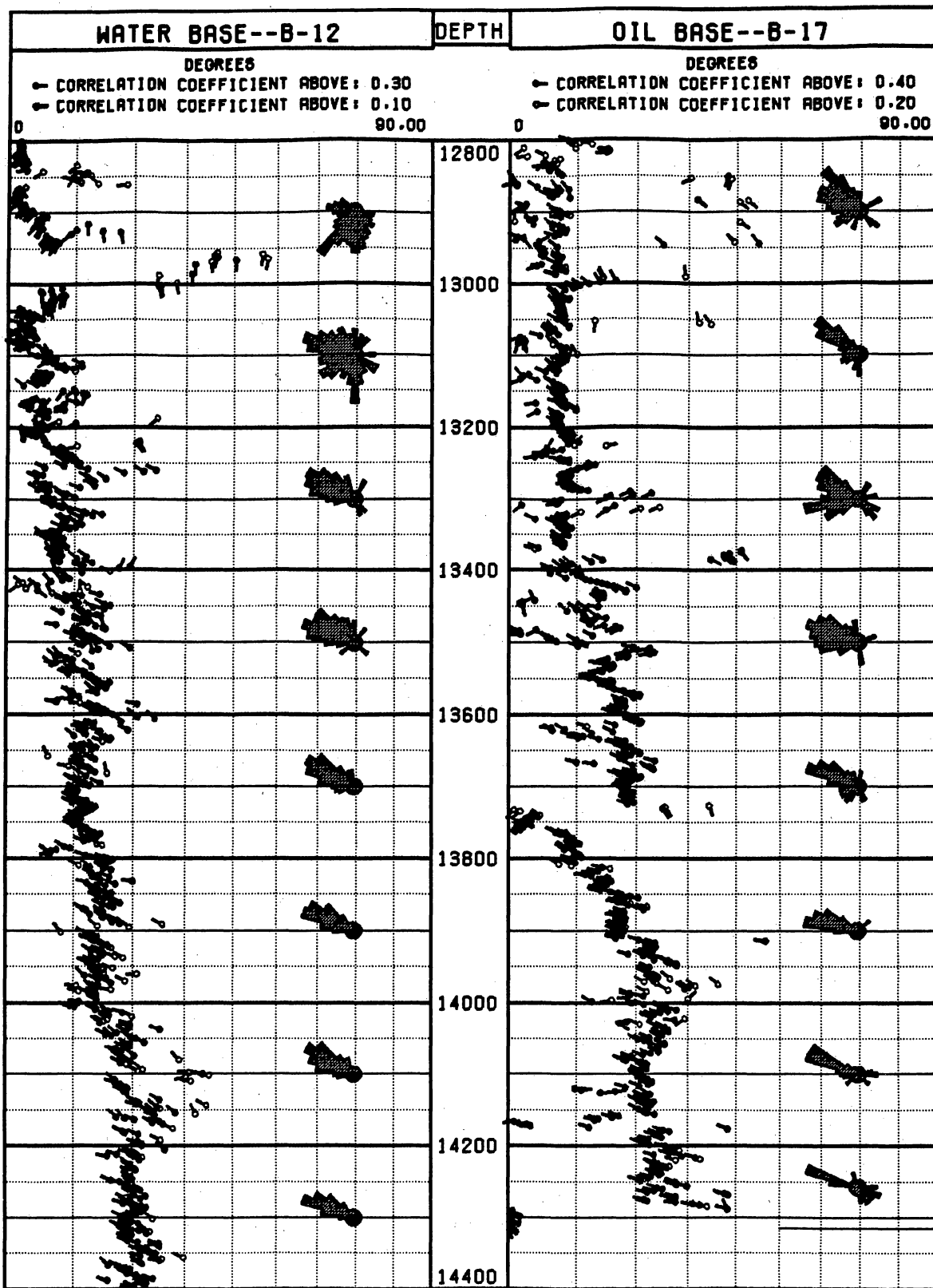
Figure 6. Comparison of water base versus oil base dipmeter results, wells B-12 and B-17.

12

PROCESSED DATA (RESULTS)

Data are subdivided into two groups based on their origin. All processed dip data were acquired from processed logs provided by the logging service company or by ResTech.

Logs processed by the logging service company were available from 10 of the wells (table 1). Data from these wells were acquired by optically digitizing prints of "tadpole plots" processed and distributed by the logging service companies. The data sets on these wells contain only a single computation of dip at each depth point, usually every 2 ft (.6 m) of well bore, plus the computed hole direction every 50 ft (15.2 m). Well B-12 has added data from a repeat section over the bottom of the well. Some wells had depth intervals for which no tadpoles were presented. This may have been due to poor acquisition data, lack of acquisition data, or poor-quality dip computations.

Original acquisition data were available on two wells plus on an additional three wells that were drilled during this study. All five wells were processed by ResTech in a manner similar to the other ten wells. These five wells were also processed to identify the orientation of hole elongation for correlation with the oriented stress determinations made on the cores (app. D). In addition, both raw microresistivity curves and dip data were extensively processed over the cored intervals of two of the wells drilled during this study for correlation between bedding structures visible in the cores and the dipmeter data. In addition to these data sets, the specially selected processing parameters, which were qualified by comparison of computed results directly with the bedding visible in the cores, are available.

DATA EDITING AND PROCESSING

The dip data processed by the logging service company were digitized optically and played back to verify the accuracy of the digitizing process. Four bits of data were digitized for each formation dip tadpole: depth, dip magnitude, dip azimuth, and dip quality. In most cases the dip quality was limited to two or three categories. In addition to the formation dip data, the hole deviation magnitude and azimuth also were digitized from a tadpole presented every 50 ft (15.2 m). These tadpoles are not assigned a quality level.

13

Raw acquisition data were obtained from five wells. These data were read from digital tapes into the database. They were first played back to verify the accuracy and completeness of the tape decoding. Calibrations of the slow channels were checked against the log prints. Any problems found at this time were corrected. Accelerometer corrections were made on fast-channel data to account for variations in tool velocity during the recording operation. The data were then processed for structural dip using two different sets of processing parameters.

Additional processing for stratigraphic interpretation was done on the five wells. Data from the two cored wells were computed using several sets of correlation parameters. The various computations were then compared with the core to identify the optimum parameters to be used on the remaining three wells. Hole eccentricity computations were made over the same intervals using the oriented dual calipers.

ACTIVITY SUMMARY

Dipmeters from 15 wells were entered into the database. Ten wells were processed by the logging service company, and five wells were processed by ResTech. A total of 58,610 ft (17,864.3 m) of wellbore is represented in this dipmeter database. The five wells with both raw and processed data represent 24,805 ft (7560.6 m) of this database. For two wells, 403 ft (122.8 m) of core is available. In addition to these dipmeter and core data, other well logs and computations make up the database.

STRUCTURAL INTERPRETATION

INTRODUCTION

Structural interpretations were made using two different sets of processing parameters. Wells B-3 through B-14 were drilled with water-based muds and computed using a 4 ft (1.2 m) correlation length, a 2 ft (.6 m) step between correlations, and a 40° search angle (4 ft X 2 ft X 40°). Wells B-15 through B-19 were drilled with oil-based muds, and the dipmeters were computed with an 8 ft (2.4 m) correlation length, a 2 ft (.6 m) step between correlations, and a 40° search angle (8 ft X 2 ft X 40°).

The change in processing parameters caused by the drilling mud and tool configuration does not appear to have influenced interpretations.

SUMMARY OF STRUCTURAL INTERPRETATION

Growth Fault Pattern

The lower portions of the dipmeters in all of the study wells display a pattern of increasing dip toward the WNW with depth (fig. 7). This pattern is the most obvious in the dipmeters of the B area and is caused by rotation of strata into a growth fault west of these wells (Marshall, 1978). This fault is a low-angle detachment surface dipping about 5°, which underlies the B area at depths of 14,000 to 15,000 ft (4,267.2 to 4,572.0 m) and is visible on seismic data. Growth fault patterns are typified by increasing dip with increasing depth, as deeper strata exhibit a greater rollover into the fault plane. Growth fault patterns commonly extend over intervals greater than 500 ft (152.4 m). In this study the patterns extend over 3,000 ft (914.4 m) in some of the wells (fig. 7).

The effect of the growth fault is to rotate strata into the fault plane and to increase the sediment thickness toward the fault. Figure 8, an E-W cross section of the "S" zone made using both

15
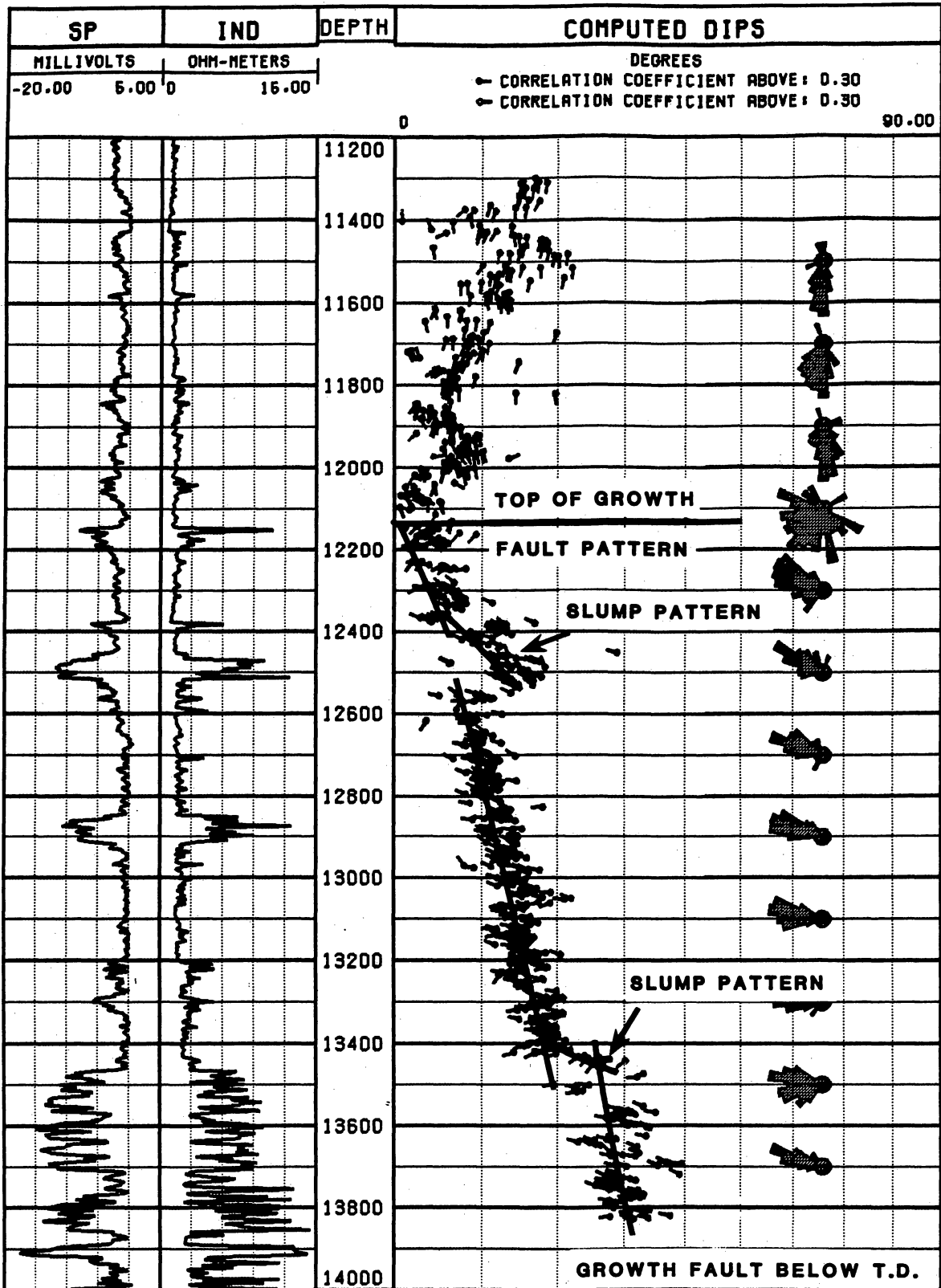
Figure 7. Typical growth fault pattern illustrating increase in dip with increasing depth: 12,300 ft - TD, well B-14.

DIPMETER CROSS SECTION--"S" ZONE

Figure 8. Dipmeter cross section showing dip increase and thickening toward the growth fault, wells B-8, B-10, B-4,. B-17, and B-14.

17

logs and dipmeters, illustrates these effects. Well B-14 on the east edge has 222 ft (67.7 m) of S reservoir. Well B-8 is approximately 2 mi (3.2 km) west toward the fault and was still in the S reservoir at TD. The S is greater than 1,870 ft (570.0 m) thick in this well and is 1,500 ft (457.2 m) lower than in well B-14.

Domains in the Growth Fault Pattern

Within the growth fault pattern, dip increases in a stepwise manner, indicating domains of relatively constant dip magnitude and dip azimuth (fig. 9). There are variations in dip magnitude and dip azimuth among the domains, both between wells and between stratigraphically adjacent domains in the same well. The domains indicate either that sedimentation was episodic or that the growth fault moved episodically, or some combination of both. The vertical lines in figure 9 indicate intervals with fairly constant dips.

Deltas are characterized by repetitive, cyclical deposition in which periods of slow deposition alternate with rapid deposition of progradational intervals (Coleman and Gagliano, 1964). Thus the dipmeters should be expected to show the effects of this periodicity. The intervals between domains, which mark fault movement, are located at the bases of upward-coarsening shale and sandstone progradational intervals at the points most likely to represent transgressive shales (fig. 10). Each domain represents the progradation of a deltaic sandstone, during which the deposition rate increases, causing an upward-coarsening sequence changing from mudstone to sandstone at the top of the interval. The horizontal lines mark points where the strata were rotated toward the growth fault.

The uppermost domain extends from the top of the S reservoir through the S_1 sandstones to the top of the S_2 sandstone. This is shown as the uppermost interval (12,880-13,100 ft; 3,926-3,993 m) in figure 11 and the two uppermost intervals in figures 9 and 10. A second domain extends through the S_2 and S_3 sandstones (fig. 11 -- 13,100-13,355 ft; 3,993-4,070 m). A third domain extends through the S_4 sandstone (fig. 11 -- 13,355-13,515; 4,070-4,119 m). Each domain represents a stratigraphic interval bounded by angular unconformities created when deposition ceased but deformation on the growth fault continued. Between deposition of the S_4 and S_3 deltas, the S_4 and

18
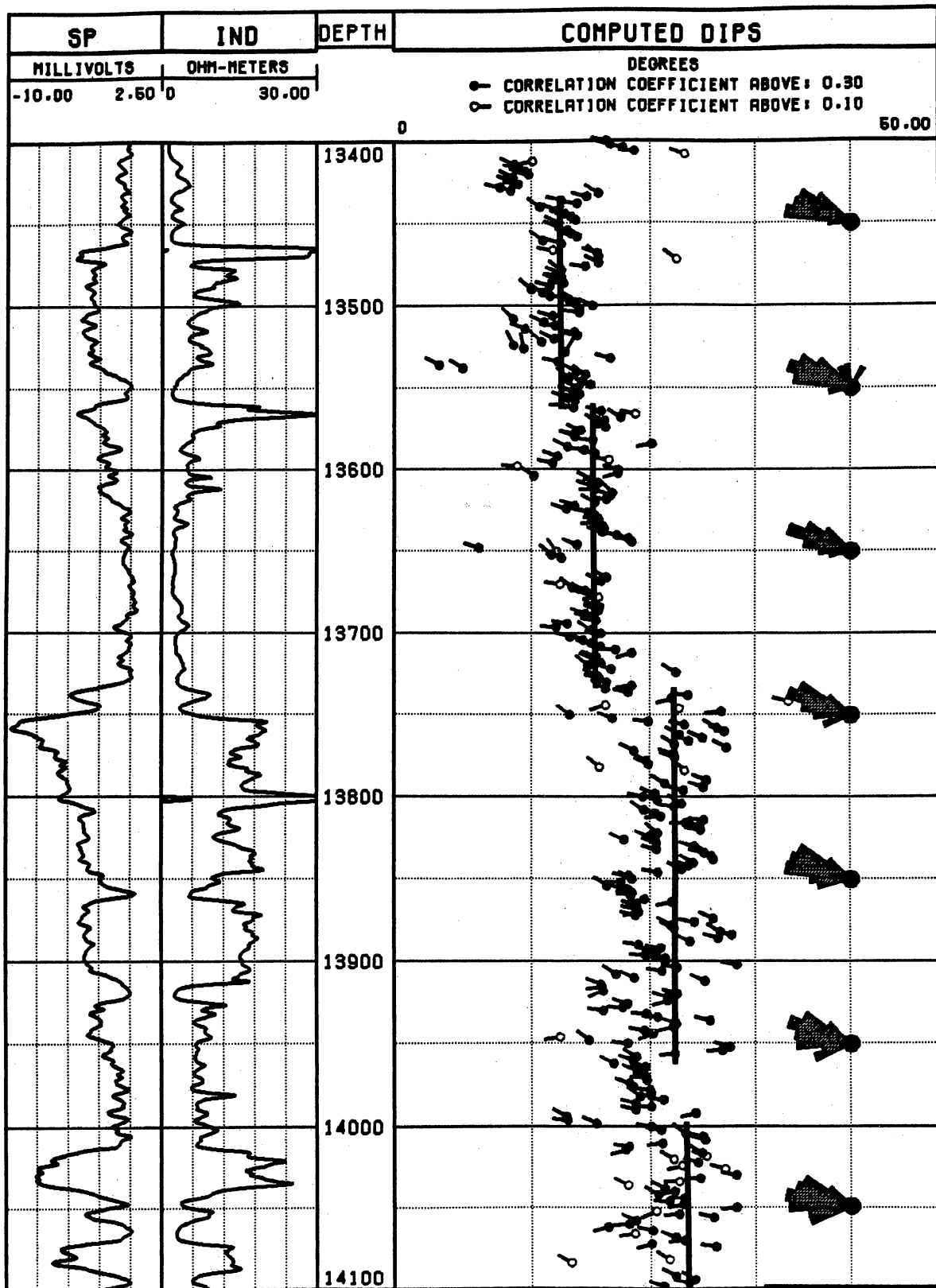
Figure 9. Dip domains in growth fault pattern illustrated by vertical lines, well B-7.

19
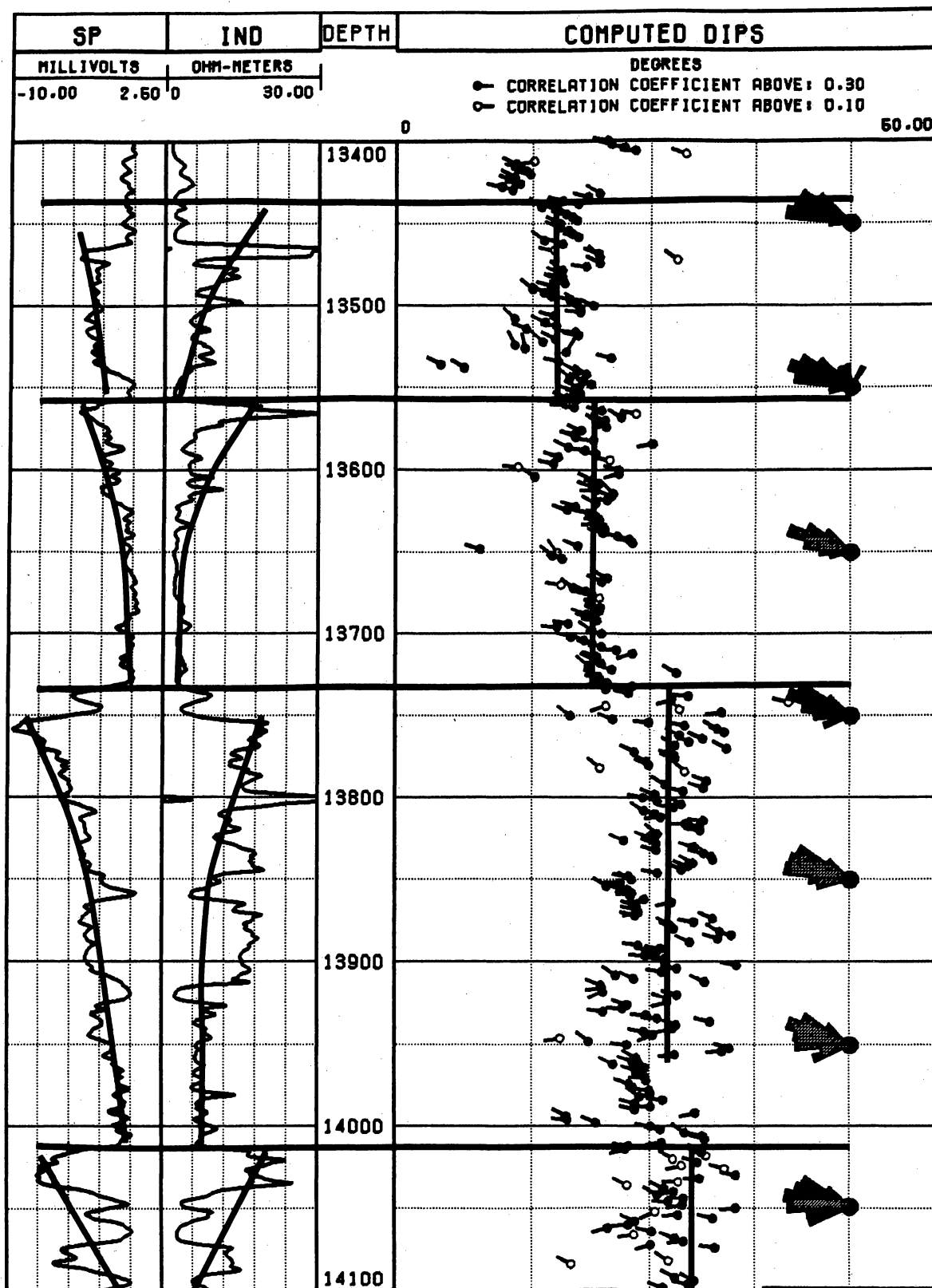
Figure 10. Correlation of sandstones to dip domains, well B-7.
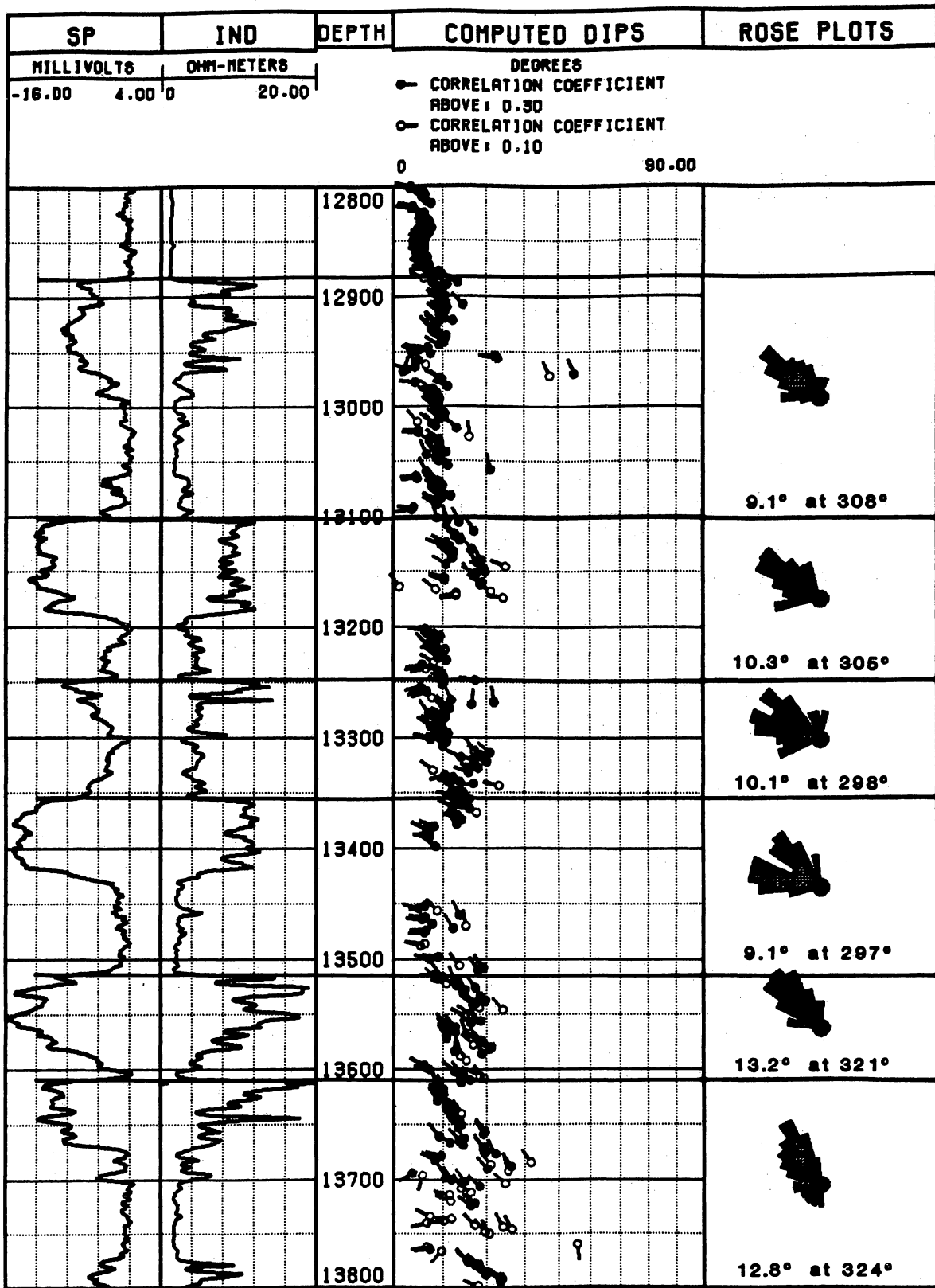
Figure 11. Azimuth variations in dip domains, well B-4.

21

underlying strata were folded along a north-south axis (3°) and also tilted down 2° to the north. Between deposition of the S_2 and S_1 deltas, the S_2 and underlying strata were folded around a north northwest-south southeast axis (333°) and also tilted down 3° to the northwest.

Dip azimuth also varies between stratigraphically adjacent domains (fig. 11). The change in the average azimuths of the dips in adjacent domains varies from 3° to 24° (fig. 11). This variation is most likely related to the direction of maximum subsidence of the fault. These azimuth variations may aid in the correlation and mapping of the individual sand/mudstone sequences and since azimuth variations reflect changes in rotation of the depositional surface, they also reflect influences on deposition.

Domains within the Same Fault Block

From the azimuths of folding along the growth faults within the B area, we can infer that it was near the center of deposition of the S_2 delta whereas, the center of deposition within the S_1 interval was farther south (Langford and others, in press). Reservoir thickness and thus the hydrocarbon content of the S_1 interval should increase to the south. Correlation of the S_1 and S_2 intervals reveals that the S_1 sandstone is thicker and is an important source of natural gas in the southern part of McAllen Ranch field and thickens from north to south within the B area (Langford and others, in press). The S_2 interval does not thicken from north to south and is an important source of natural gas in both the B area and the southern parts of the fields. Used in this manner, the thicker and thus more prolific portions of gas reservoirs may be located using dipmeters and stratigraphic correlation.

Location of Faults Between Wells

Additionally, although it contains the same domains, the B-3 well exhibits different axes of rotation. When the effects of rotation on the S_1 interval are removed, dips in the B area wells are perpendicular to the axis of folding. The B-3 well is the exception and its dips diverge from the other wells indicating it is influenced by a second growth fault that was active during deposition. Examination of the map of the field indicates this additional fault probably extends east-west between the B-3 and

the other B area wells that was not mapped in our original effort (figure 2). The location and orientation of this fault has been confirmed by three-dimensional seismic data (Hill and others, 1991).

Stratigraphic correlation of domains.

Analysis of the B-5 well in the northeastern corner of the B area reveals significant differences from the rest of the wells, including the B-3 well. There are no obvious dip domains within the growth fault pattern of the B-5 well. Originally the B-5 well had been interpreted as a continuation of the Vicksburg S reservoir in a different fault block. However, as is seen in analysis of the B-3 well, since the S reservoir was created through progradation of the same 6 deltas, even though a reservoir is cut by a growth fault, it should contain the same number of dip domains, although the azimuths of these domains may be different. Since the B-5 well contains no dip domains, and since stratigraphic correlation of the sandstones is uncertain, the B-5 should be interpreted to be part of a different reservoir, stratigraphically above the Vicksburg S reservoir. It was this reinterpretation that resulted in a successful drilling campaign by Shell Western E. & P. into the previously inferred fault gap between the B-5 and the rest of the B area wells (Hill and others, 1991). In figure 4 this is the gap between the #B-5 and #B-52 wells and the #B-1 and #B-8 wells.

Other Faults

Dipmeters detect faults by detecting the rotation and deformation of strata on either side of faults. A fault with movement that does not contain some component of rotation or deformation of strata cannot be detected by a dipmeter. The fault-associated deformation that is most easily detected by dipmeters is drag and slumping in strata immediately adjacent to the faults. This deformation records the direction of movement along the fault and in many cases allows inferences to be made about the dip and azimuth of the faults. In some wells in the B area rotational patterns are interpreted as drag associated with normal faults. It was assumed that drag rather than slumping produced the rotation because these were clearly postdepositional high-angle faults, and slumping is unlikely to be significant in these instances. In addition, features in two faults cored in wells B-18 and B-17 indicated that drag is more

23

likely to occur. These post depositional faults are difficult to infer from dipmeters. One fault was cored in the B-17 well at 12,720 ft (3,877 m) but this would have been impossible to infer from patterns within the dipmeter.

The rotational patterns indicate down-to-the-west displacement. The dipmeters also contain fault patterns higher in the section (at approximately the L and R horizons) striking ENE-WSW and down to the SSE. The stratigraphically higher faults do not correlate with displacement within the S reservoir, and displacements on these faults cannot be related to structure within the S. It is therefore assumed that these higher faults are listric and die out within the thick shales between the R and S horizons.

Unconformity

The dip of strata immediately above the "S" zone was determined by making azimuth frequency plots of the interval directly above the S reservoir (fig. 12). The interval from 13,800 to 13,850 ft (4,206.2 to 4,221.5 m) in fig. 12 should be close to the dip of the surface of the S reservoir at 13,872 ft (4,228.2 m) if the S reservoir and overlying shales are conformable. This interval was plotted on a modified Schmidt plot and the dips were averaged. The average dip values were computed for all wells. The Schmidt plot displays azimuth around a circle and dip as distance away from the center of the circle. Steeper dips plot nearer to the center of the circle.

In some cases fault noise in the dipmeter caused these results to be suspect. However, the structural dips derived from the dipmeter were compared with the structural dips output from a computer mapping program based on well correlation of the top of the S reservoir. A special dip plot was used to compare the map dips with the dipmeter dips (fig. 13). This plot separates the dip magnitude and the dip azimuth, and it plots each as a point. The dip magnitude is plotted in Track 1 as DIP. The dip azimuth is plotted in Track 2 as AZIM. The map dip is plotted as dashed lines with the dip magnitude (MDIP) in Track 1 and the dip azimuth (MAZIM) in Track 2. This plot allows easy comparison of dipmeter data with well-to-well correlation data, which was done for each of the wells.

These plots revealed a substantial angular discordance between the S reservoir and the overlying shales (figs. 13, 14a and 14b). The dip of the overlying shales is generally smaller and more

24
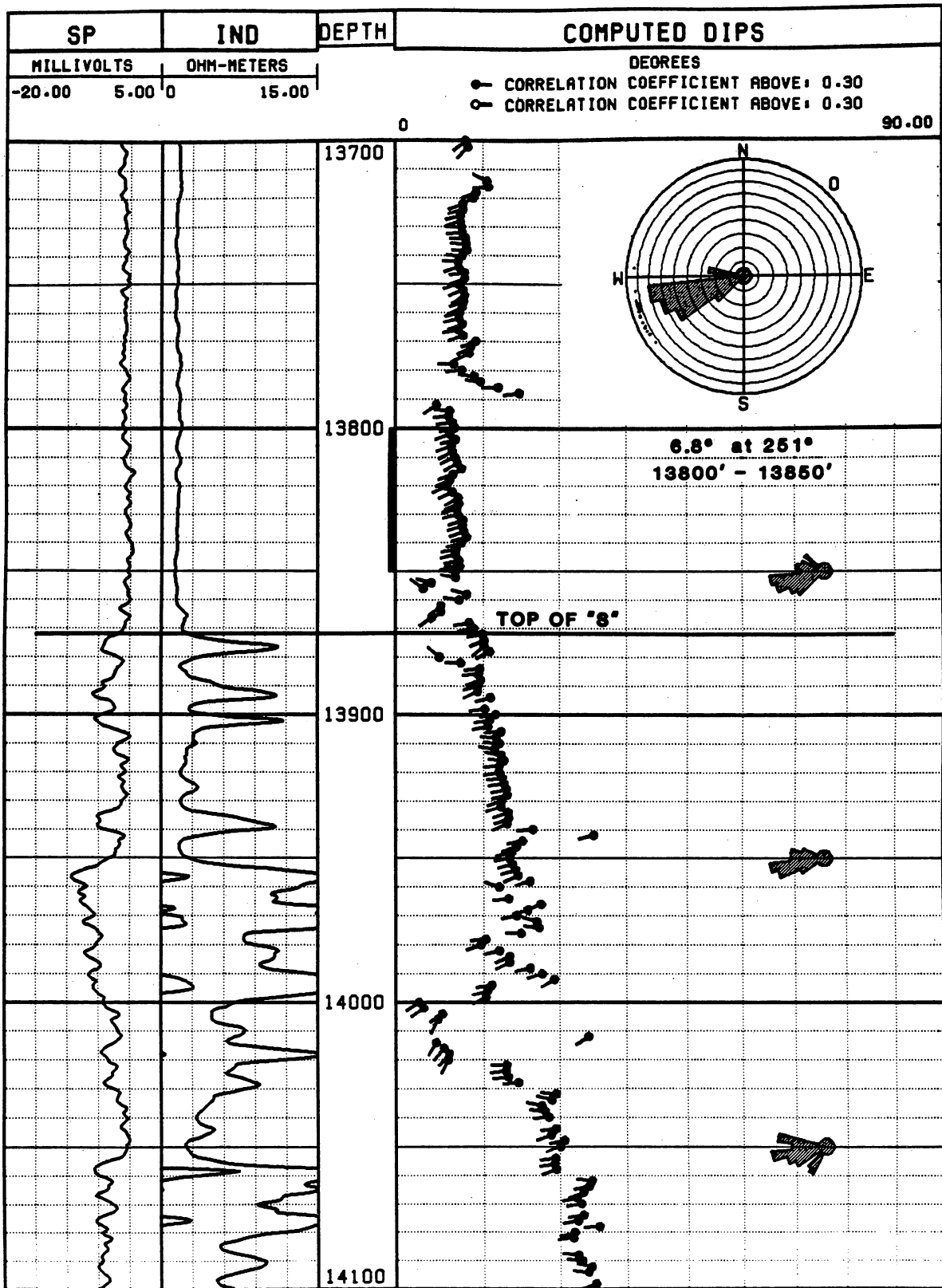
Figure 12. Structural dip at the base of the "R" zone, well B-8.
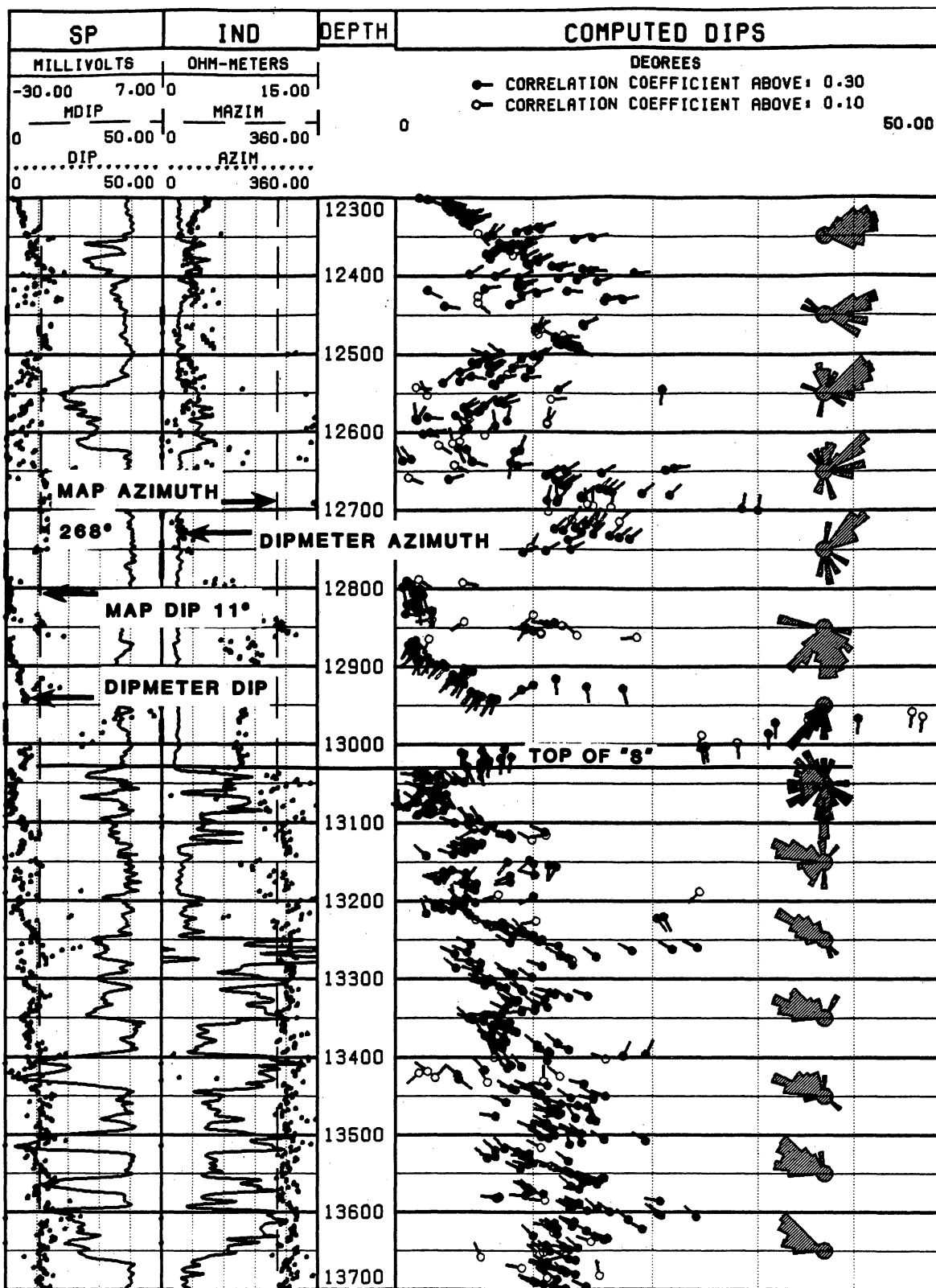
Figure 13. Comparison of map dip on top of the S reservoir with dipmeter dips in base of the "R" zone, well B-12.

26

(a)

DIP MAGNITUDE FROM MAP

DIP MAGNITUDE FROM DIPMETER

(b)

DIP AZIMUTH FROM MAP

DIP AZIMUTH FROM DIPMETER
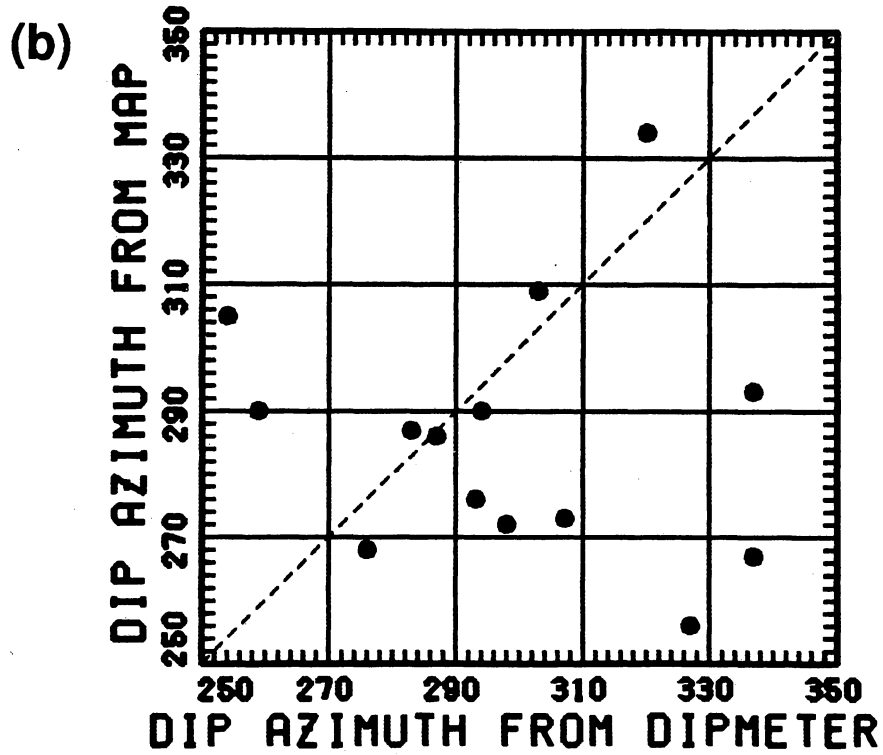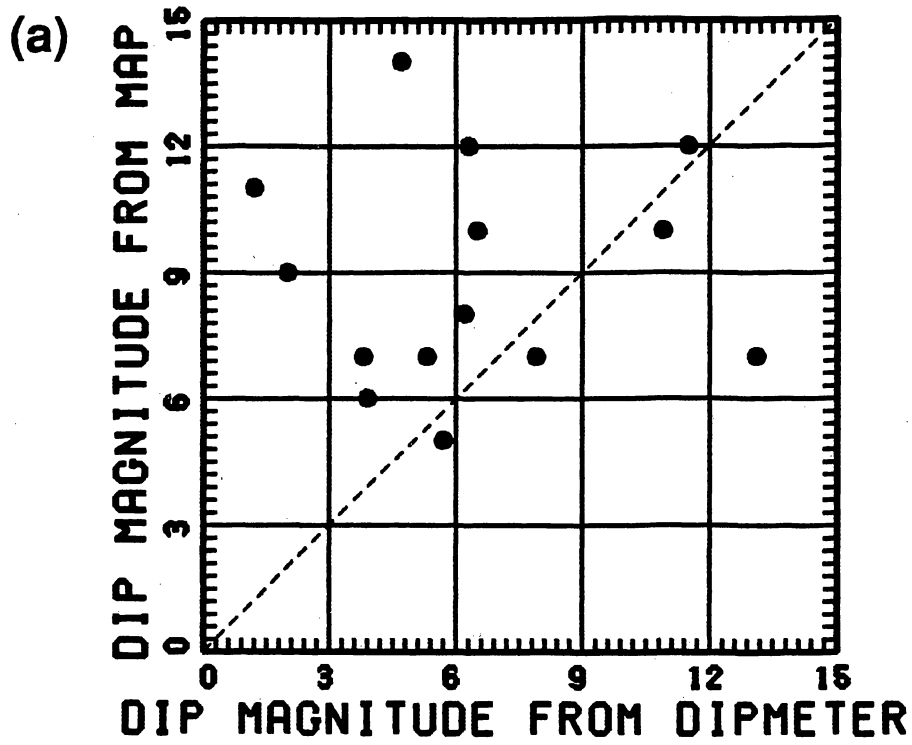
Figure 14. (a) Comparison of dip magnitudes from dipmeter with those from map.
(b) Comparison of dip azimuths from dipmeter with those from map.

northwesterly than the steeper, more westerly dips at the top of the S reservoir. Fig. 14a indicates that the dip magnitudes from the dipmeter are generally lower. Fig. 14b indicates that the dip azimuths from the dipmeter are generally more northerly than the map dips. The comparison between the dips within the S and the interval immediately above it indicate that the S reservoir in the B area was folded along a northwesterly axis (330°) and tilted down 2° to the north prior to deposition of overlying strata.

Slump Patterns

Many deflections occur within the overall upward decrease in dip associated with the fault rotation (fig. 15). These are dip patterns of constant dip azimuth but sharply increasing dip magnitude with increasing depth and are interpreted as resulting from soft-sediment deformation following early deposition. They are termed slump patterns. Slump patterns range in thickness from less than 6 inches (15.2 cm) to more than 100 ft (30.5 m) and are pervasive within the intervals rotated by the growth fault.

Most of these slump patterns indicate rotation of the deformed interval down to the east. Although many types of soft-sediment deformation or fault deformation could produce this pattern, their association with specific stratigraphic intervals and their similarity suggest a common origin. Our favored interpretation is that the slump pattern represents rotation of soft sediment along listric faults as rotational slump blocks (fig. 15). In most cases the rotation is to the east, indicating westward movement toward the growth fault. If these features are in fact slumps, they provide a means of reconstructing the deformation along the growth fault.

Fig. 16 shows an interval of rotation interpreted as a possible slump in well B-17 that extends from 13,725 to 13,980 ft (4,183.4 to 4,261.1 m). This pattern can be correlated with displacement on the vertical seismic profile. Fig. 17 shows a 20 ft (6.1 m) rotation in well B-17 that extends from 13,618 to 13,638 ft (4,150.8 to 4,156.9 m). Fig. 18 shows a slump pattern in well B-15 that extends more than 1 ft (.3 m). These three slumps illustrate the wide variation in slump size that can be identified on these dipmeters. Fig. 19 shows slump patterns of various sizes in a single well. At 14,050 ft (4,282.4 m) is an example of a 10 ft (3.1 m) slump pattern within a 100 ft (30.5 m) slump pattern. Slump patterns tend to

(a)

Inclination

0   5   10   15

Vertical scale from 2 to 500 ft

(b)

QA 15550c
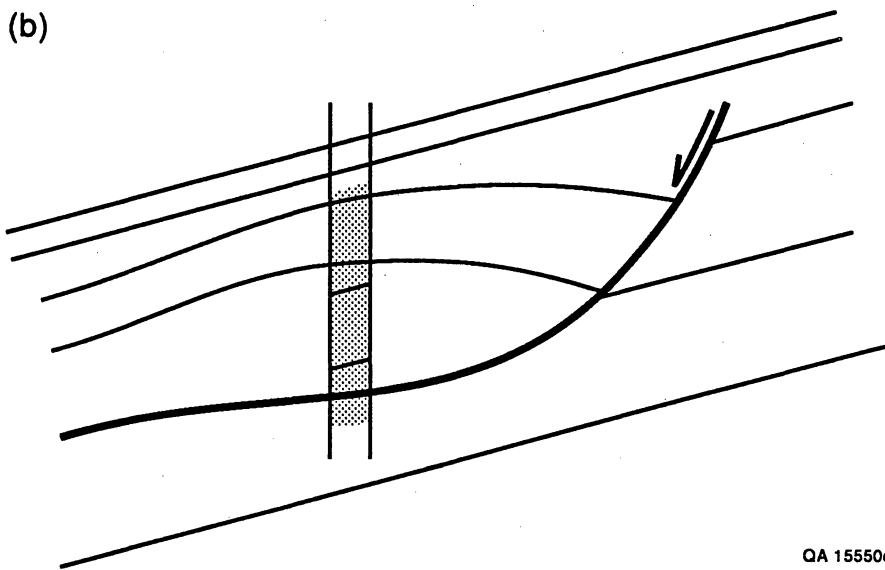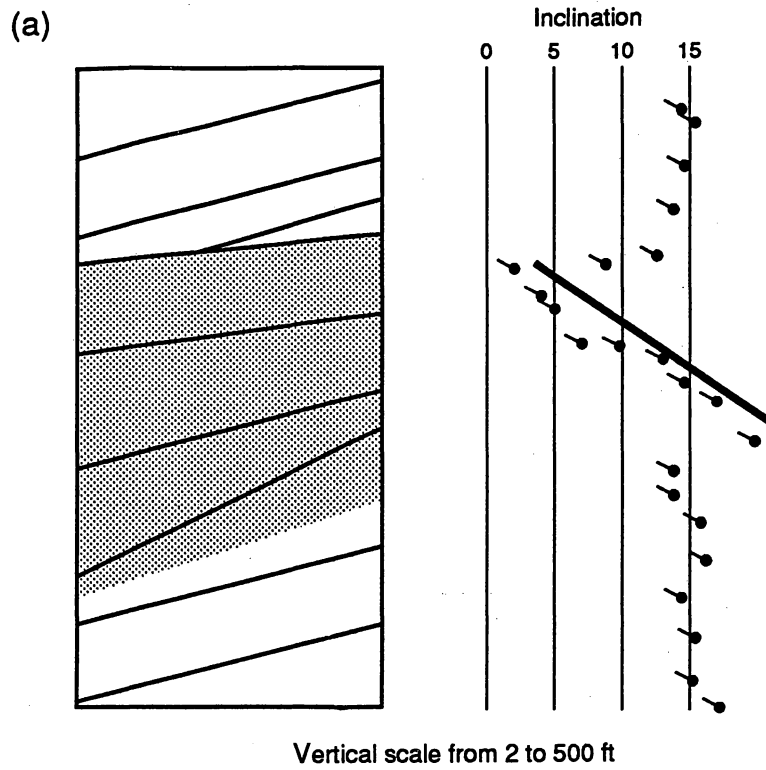
Figure 15. (a) Diagram showing the pattern observed in dipmeter logs and corresponding strata in well bore.

(b) Geological interpretation of this pattern as a rotational slump.

29
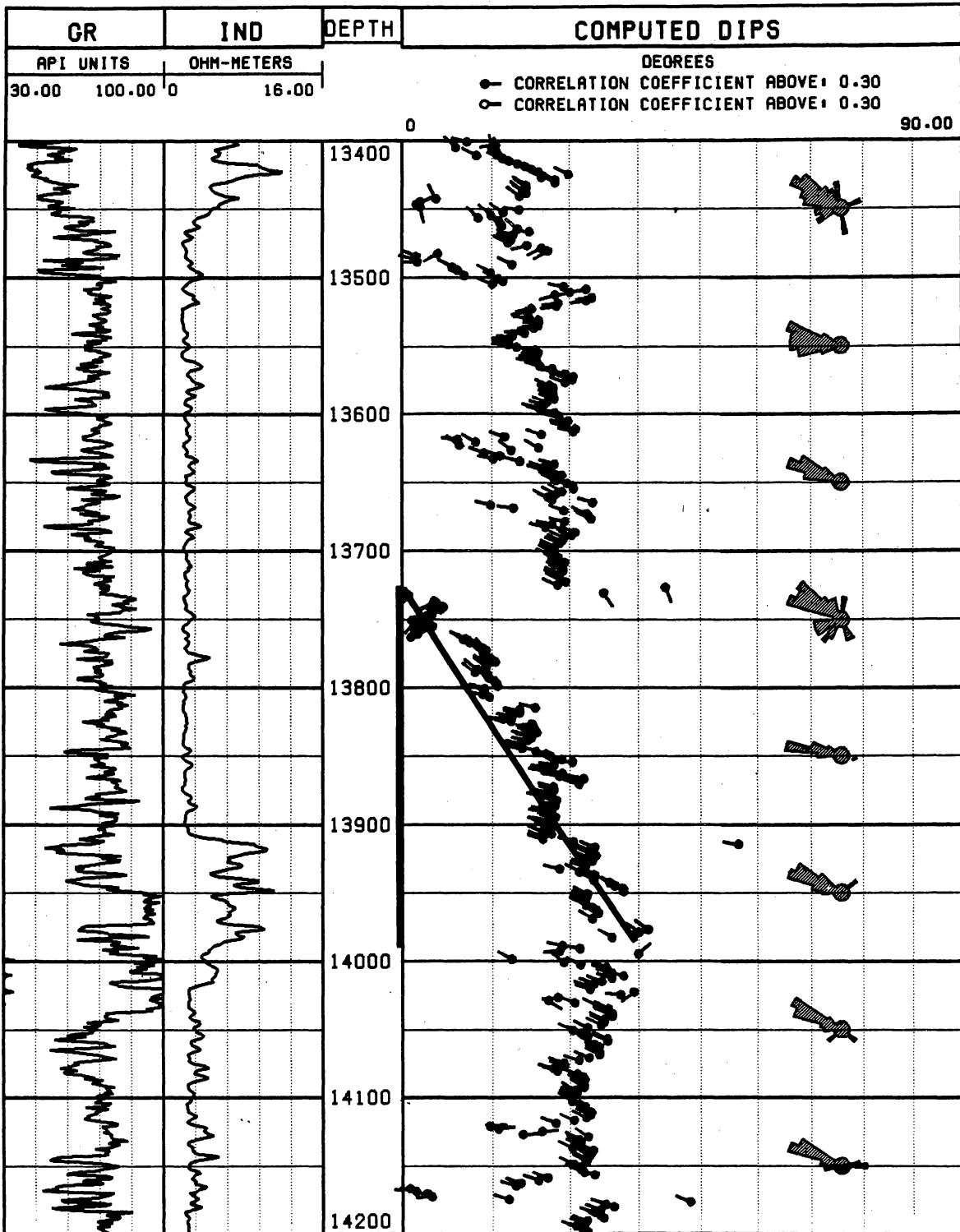
Figure 16. Example of large rotation interpreted as a slump (> 200 ft.) 13,775 to 13,980 ft., well B-17.
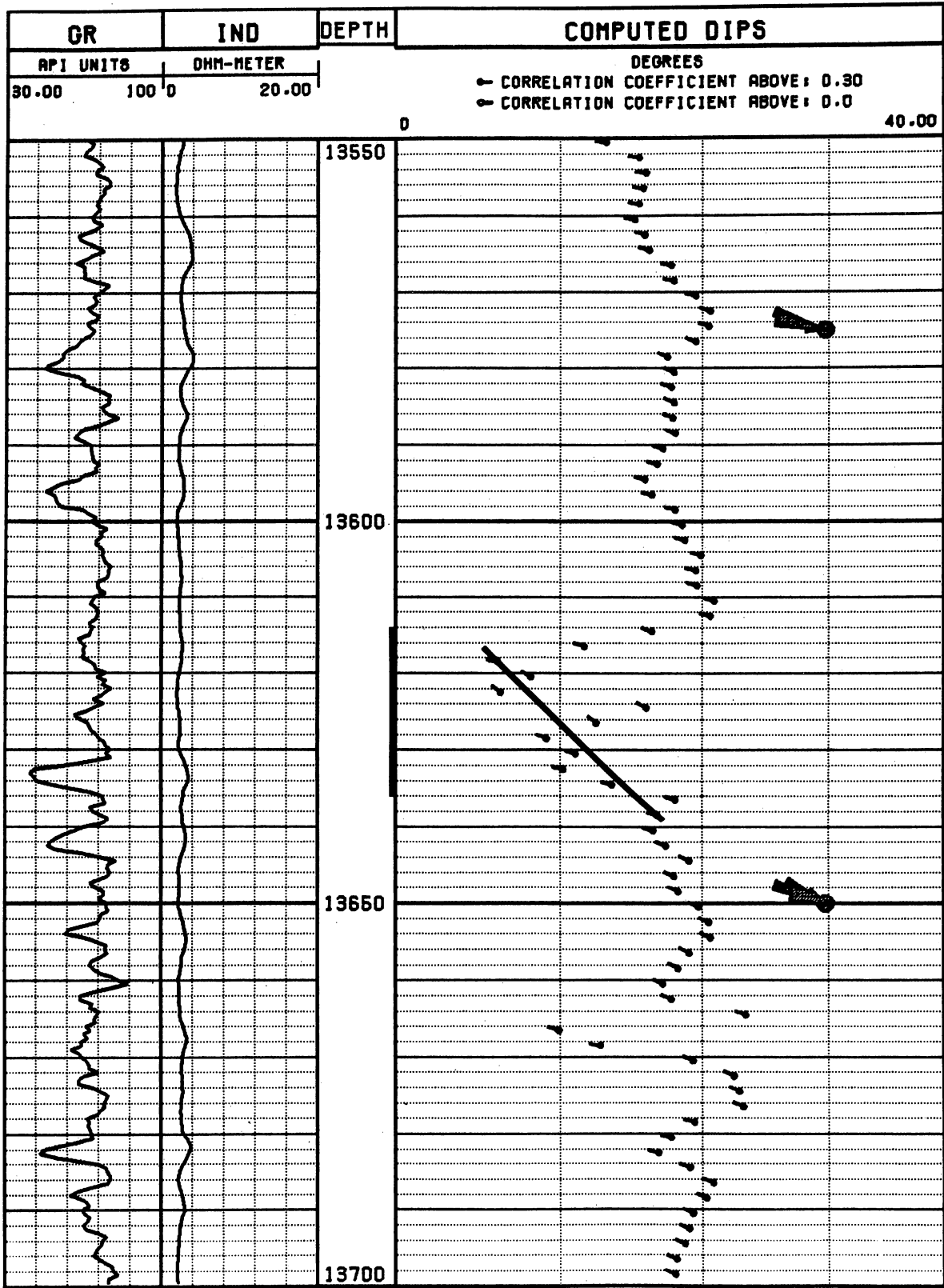
Figure 17. Example of medium rotational feature (20 ft.) 13,616 to 13,636 ft., well B-17.

31
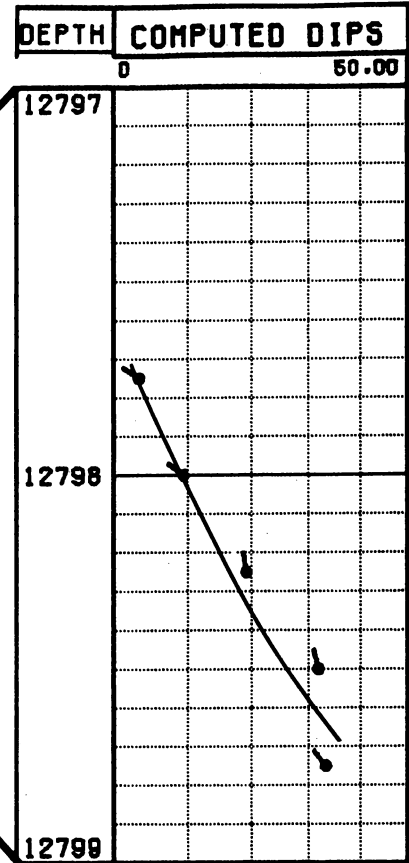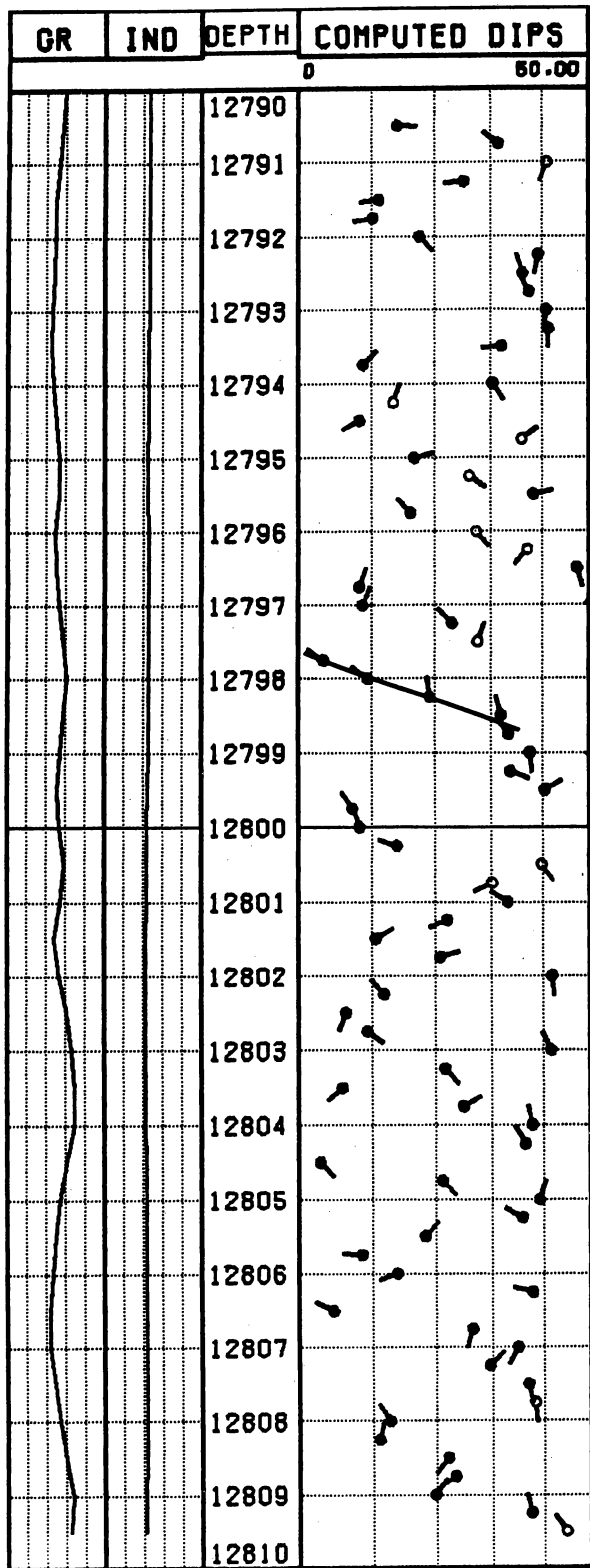
Figure 18. Example of short interval interpreted as a slump feature (1.2 ft.), well B-15.

SP	IND	DEPTH	COMPUTED DIPS
MILLIVOLTS	OHM-METERS		DEGREES
-30.00 7.50	0 20.00		CORRELATION COEFFICIENT ABOVE: 0.30
			CORRELATION COEFFICIENT ABOVE: 0.10
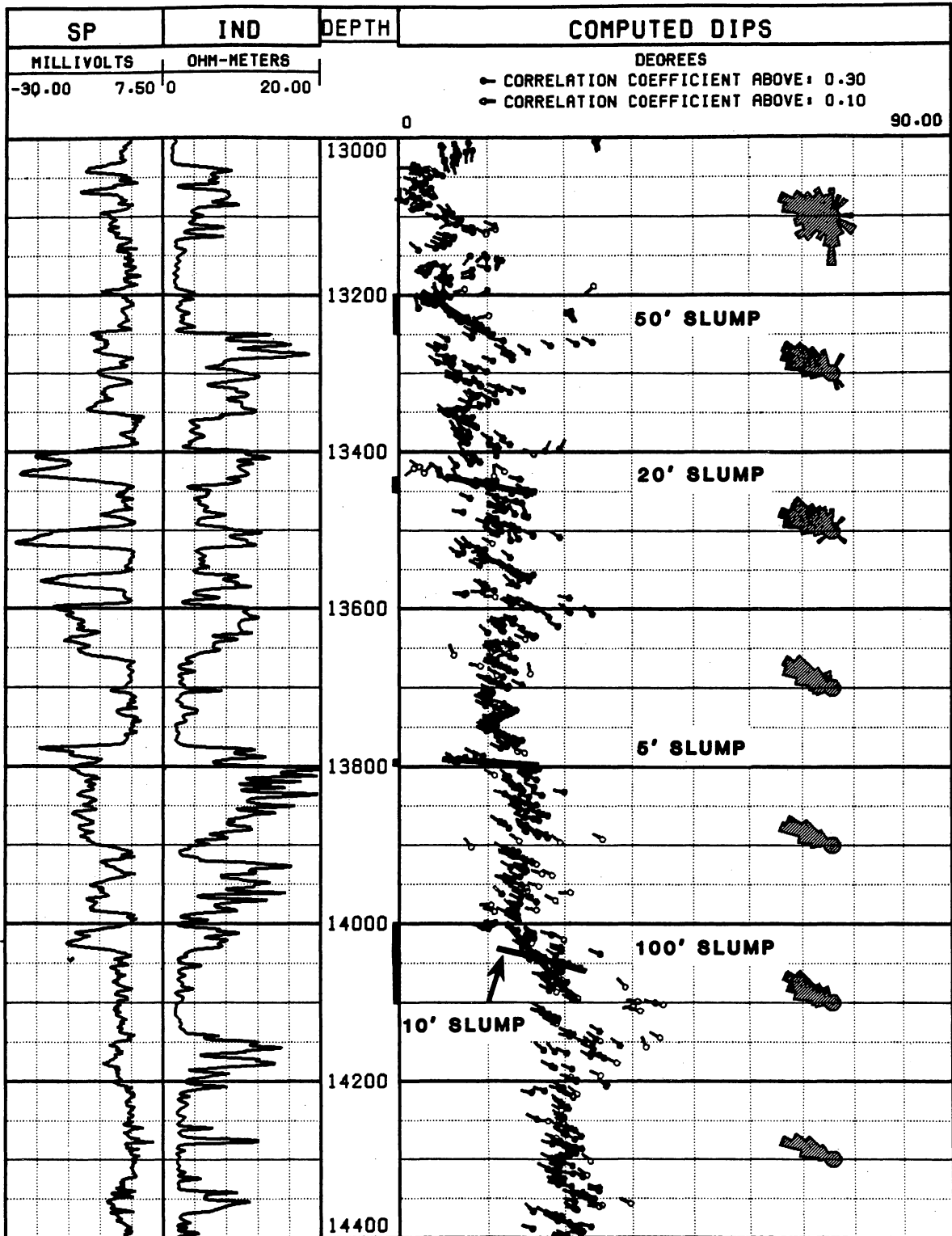
Figure 19. Different sizes of rotations, well B-12.

33

occur at or near the top of the progradational sandstone intervals. Fig. 20 shows this correlation in well B-12.

Slumps are important for this study in that they represent a potential source of heterogeneity within the S reservoir. Because the S reservoir completions are commingled, there is no way of quantifying the degree to which these possible slumps may impact gas flow within the reservoir. However, when considering potential types of permeability barriers within other fields, the possible occurrence of slumps should be evaluated.

Rotation on the Growth Fault

Rotation by the growth fault gradually dies out upward within the dipmeters. Figure 21 shows how rotation tapers off at 12,000 ft (3,520.4 m) in well B-7. The top of the interval affected by the growth fault can be fairly accurately picked by extrapolating the dip pattern in a straight line to a low dip value. Most wells show a reduction in dip magnitude followed by a change in dip azimuth toward the south. Figure 22 shows the abrupt change of the azimuth in well B-4. Figure 23 is an azimuth vector plot of the same data from 11,800 to 12,100 ft (3,596.6 to 3,688.1 m) showing the magnitude of the azimuth change to be about 80° in this well. The azimuth vector plot displays dip azimuths as connected vectors from bottom to top of an interval. Since dip magnitude is not involved, scale is not shown on this plot, only direction.

This point was thought to be a possible marker bed since it appears to mark a structural change, but the intervals bear no relationship to stratigraphy. The change in dip at different stratigraphic intervals within closely spaced wells illustrates the complex structural history at McAllen Ranch. It indicates the interplay between westward rotation toward the growth fault and northward rotation across the entire field, which dropped the B area relative to the southern parts of the S reservoir (fig. 2). Table 2 lists the current depths and dip values in all of the wells.

Fig. 24 shows azimuth frequency diagrams of the "S" zone displayed on a map. The dip azimuth changes from WNW in the southeast portion of the field to NNW in the northeast portion of the
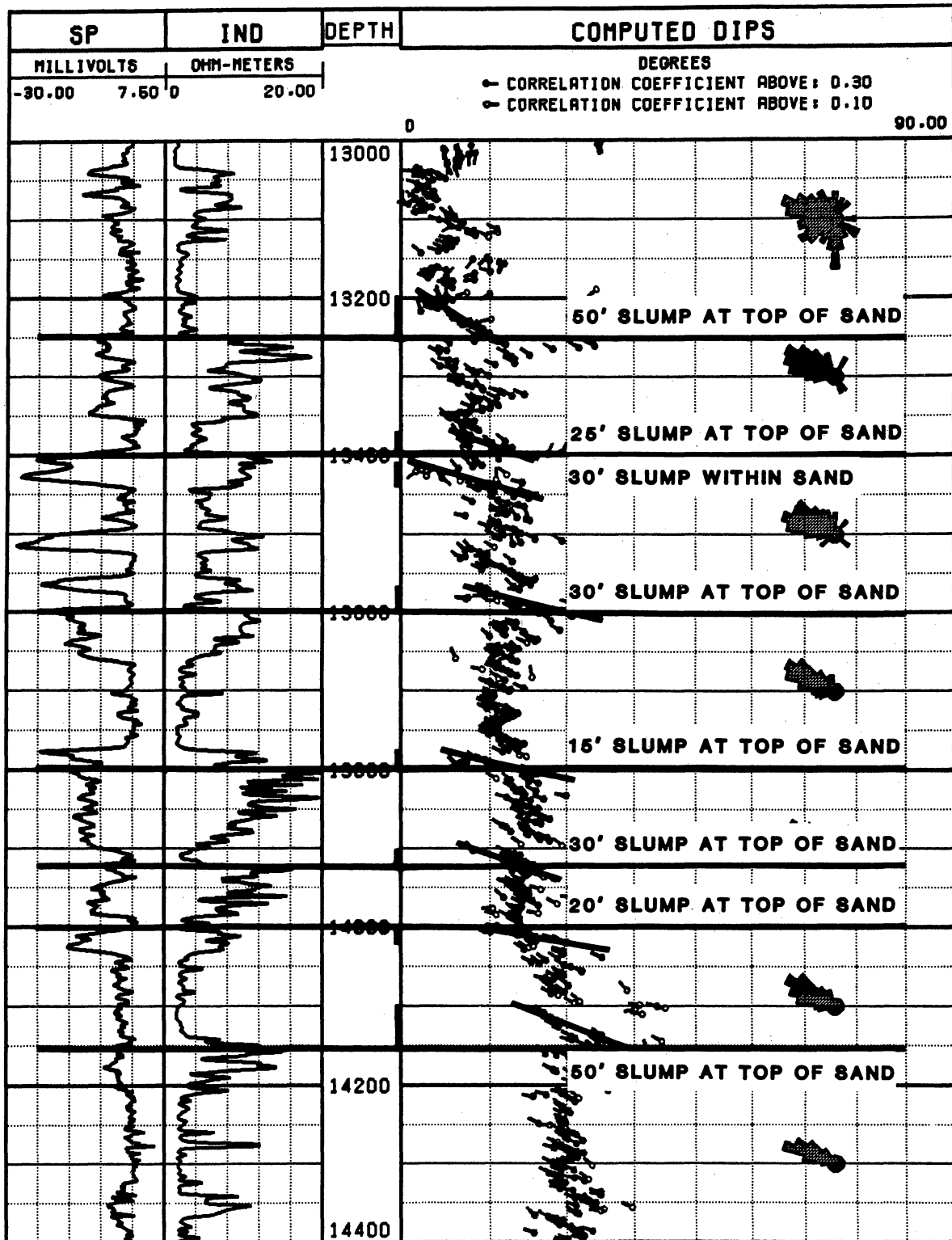
Figure 20. Correlation between rotational "slump patterns" and sandstones, well B-12.
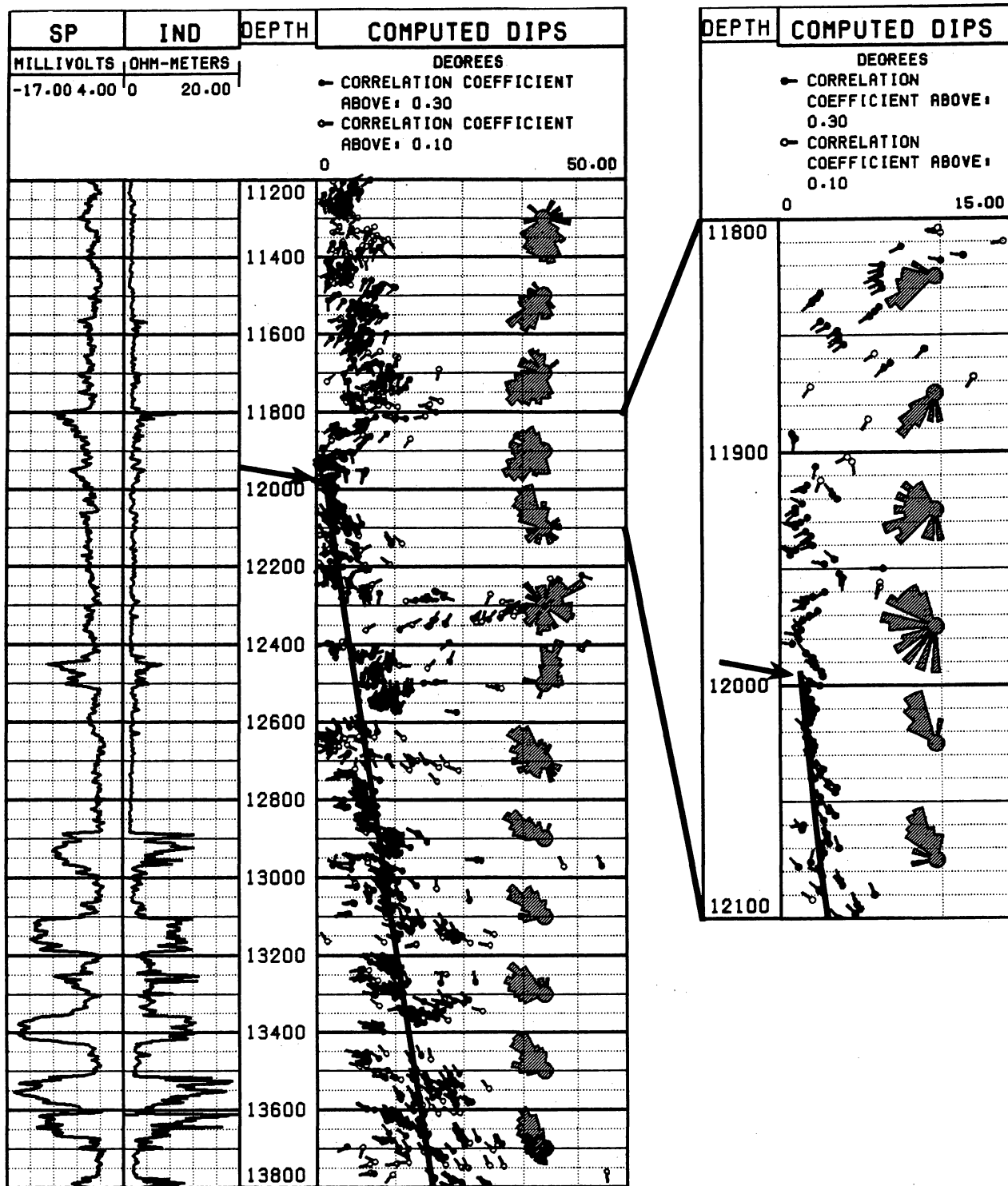
Figure 21. Top of interval rotated by growth fault, well B-7.

36
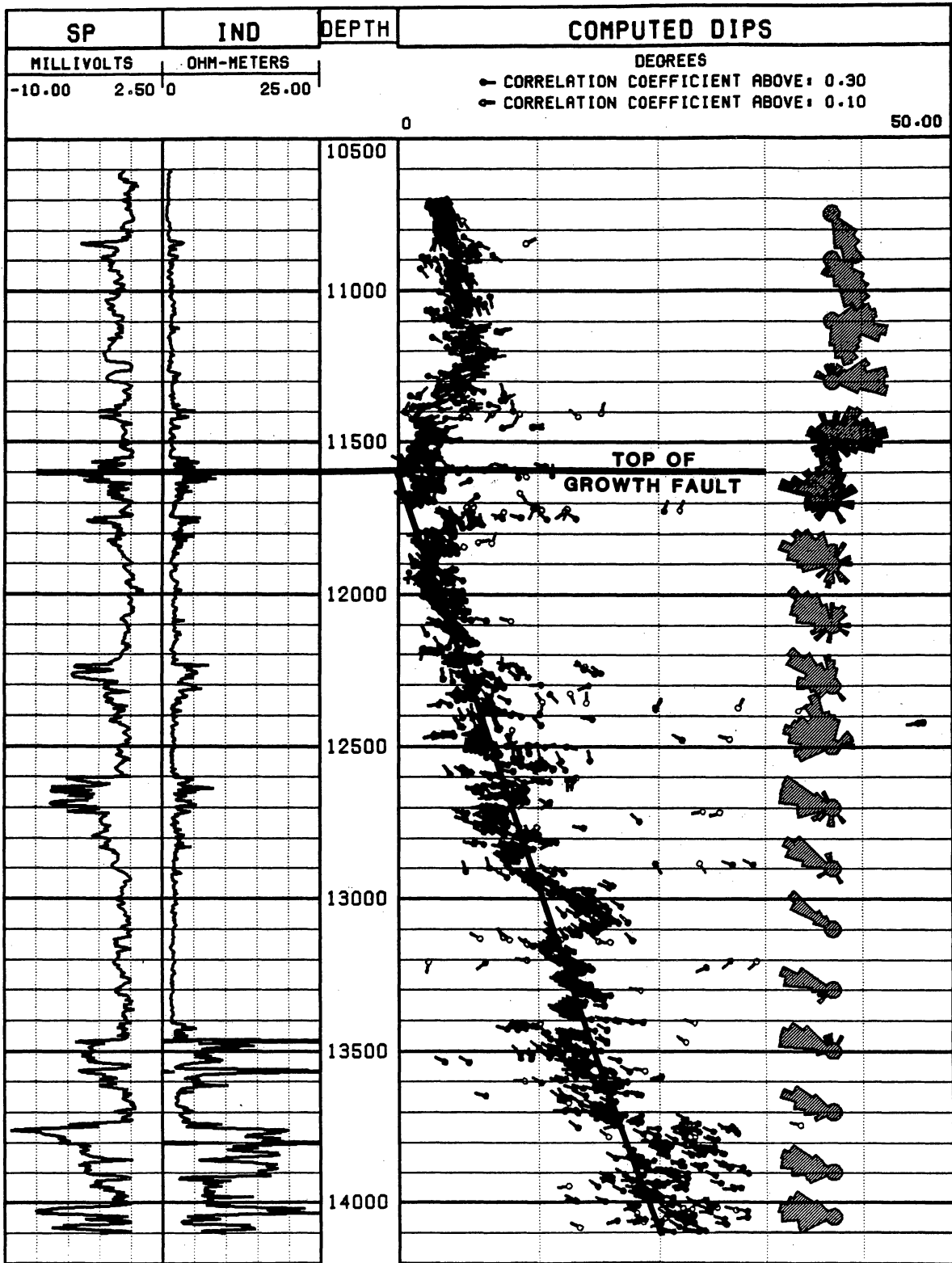
Figure 22. Change in dip azimuth at top of growth fault rotated interval 11,975 ft., well B-4.
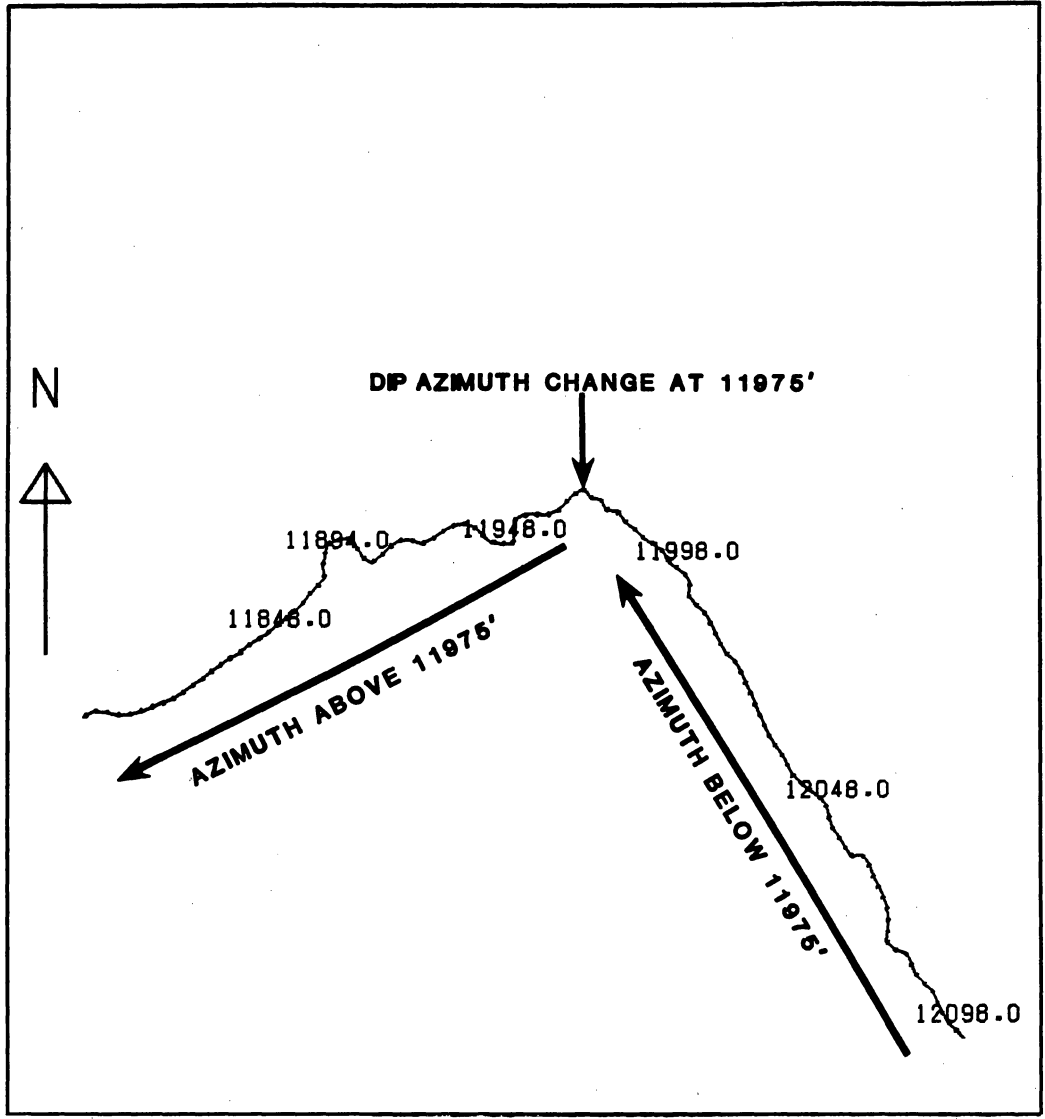
Figure 23. Azimuth vector plot showing abrupt change in dip azimuth at top of growth fault rotated interval, well B-4.

Table 2. Depths of dip azimuth change.

Well name	Depth (ft)	Dip magnitude (°)
B-3	11,400	8.0
B-4	11,920	1.0
B-5	11,250	10.0
B-6	12,760	1.0
B-7	11,555	1.0
B-8	12,310	2.0
B-10	12,040	0.5
B-11	11,550	1.0
B-12	13,035	1.0
B-14	12,250	2.0
B-15	12,425	4.0
B-16	11,920	1.0
B-17	11,795	1.0
B-18	11,850	2.0
B-19	12,280	1.0
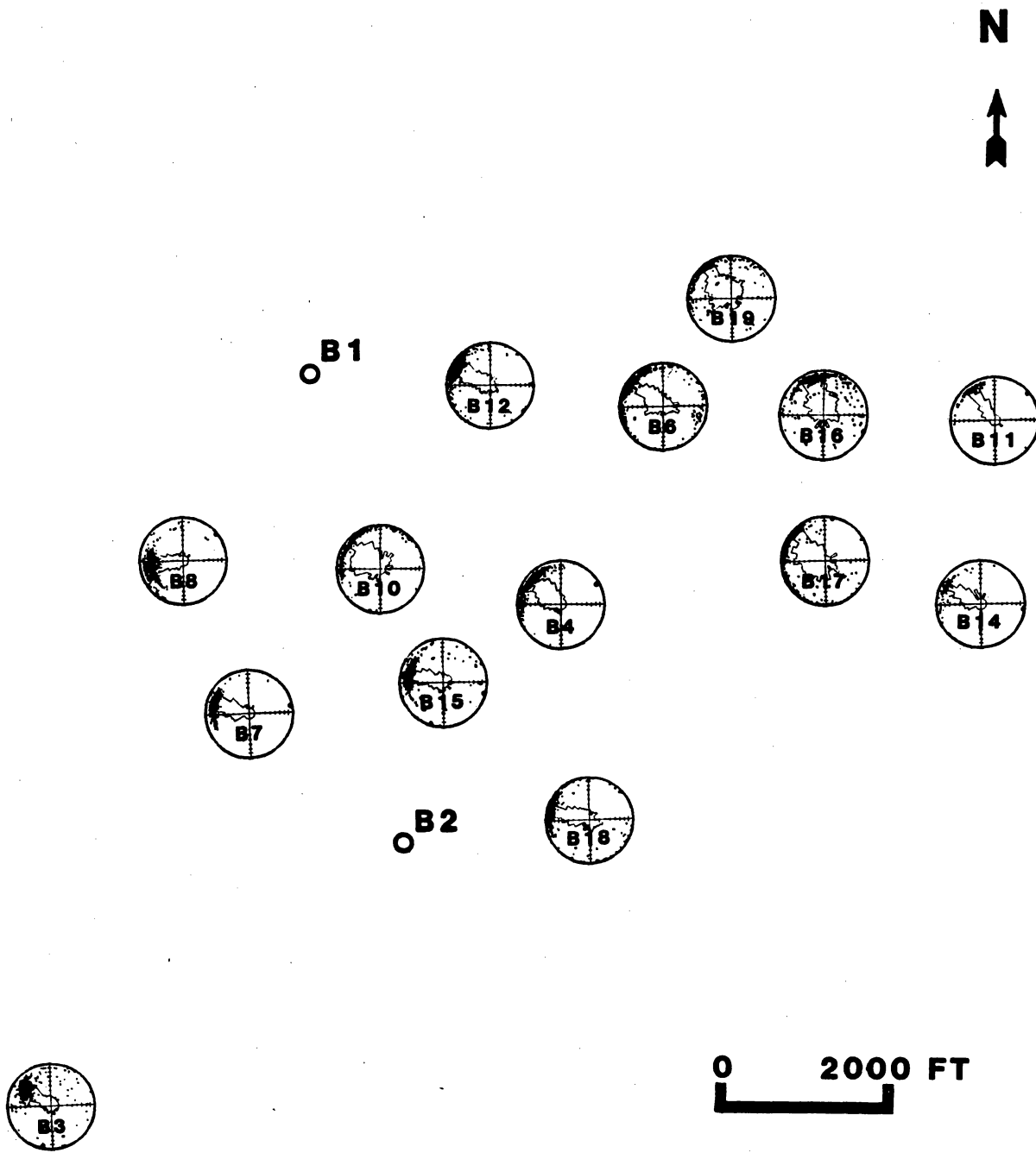
Figure 24. Azimuth frequency diagrams of S reservoir.

field. The dip magnitudes increase from east to west toward the growth fault. The dip azimuths are more dispersed or have a wider frequency diagram in the central and north portion of the field. The northerly component of the dips is not reflected in well-to-well correlation within the S interval. This indicates that there is structural complexity on a scale smaller than the faulting. The northwesterly dips observed might result from a combination of rotation to the west into the growth fault and rotation to the northeast along a series of three small faults oriented NW-SE that occur in the northeast part of the B lease (figs. 2 and 24).

HOLE ECCENTRICITY INTERPRETATION

INTRODUCTION

Determining the direction of fracture propagation within the S reservoir is important for natural gas recovery in low permeability reservoirs because induced hydraulic fractures may breach permeability barriers, depending on orientation. Fracture propagation may be inferred from determination of in situ stress in the reservoir. Fractures grow parallel to the direction of maximum horizontal compressive stress. The results of this study were used to create a model of the S_4 reservoir in which we attempted to quantify the magnitude of permeability barriers within the S reservoir (Langford and others, in press).

Since the introduction of four-arm calipers as an adjunct to dipmeter recordings, the orientation of hole elongation has been examined in conjunction with in situ stress data in an effort to predict formation stress vectors. Although it is recognized that hole elongation correlates with stress vectors, other factors must be considered when making interpretations, including amount and direction of hole deviation, drilling assemblies (including bits and stabilizers), structural dip of the formation, tectonic history of the area, orientation of the reservoir, and drilling fluids. All of these factors can influence the azimuth or degree of hole elongation. In addition, the four-arm (or six-arm) dipmeters may not always align the calipers so that at least one of the pair of calipers is oriented with the longest axis of the hole. This often occurs when the degree of hole elongation is small. It is always a factor when the tool is rotating, which is common when hole elongation is small. The four-arm caliper can measure only two perpendicular diameters, and if the hole cross section is not symmetrical with the axes of both calipers, it is possible that elongation due to formation stress can be obscured by hole elongation due to a directional hole or other influences. Thus it is important to examine the data from each well in context with the total data set from all wells when making interpretations.

43

PROCESSING AND PRESENTATIONS

Caliper data are available from five wells (wells B-15 through B-19) (fig. 4). The caliper data were processed by comparing the difference between caliper diameters with the smallest caliper diameter. This value was computed every 3 inches (7.6 cm) of well bore over the S reservoir. The azimuth of the widest caliper dimension was computed and the data plotted in the same formats that are used when plotting dip magnitude and azimuth, except in this case the value of hole elongation was substituted for dip magnitude and the azimuth of the long diameter was substituted for dip azimuth (fig. 25). Schmidt diagrams over the processed interval were used to identify the orientation of the major hole elongation. Figure 25 is a special presentation of hole elongation using an adaptation of the dipmeter presentation. In this presentation the "tadpole" has two tails, which are aligned with the largest caliper (long axis of the hole). The center of the tadpole reads a "dip" value that is proportional to the hole elongation. This presentation allows hole elongation, orientation of the long axis, and depth to be displayed with a single character. Fig. 26 is a Schmidt plot that has been modified to reflect both the azimuths and the magnitude of the hole elongation, which increases toward the center of the plot. This "propeller plot" was used to compute the azimuths of the hole elongations over the S zone on all wells where caliper data were available. These data were plotted on a map and compared with the azimuths of the acoustic anisotropy measurements made on the core from well B-18 (fig. 27). For a discussion of acoustic anisotropy measurements of formation stress see appendix D.

INTERPRETATION OF RESULTS

The azimuths of hole elongation from the five wells trended NW-SE (table 3). This is interpreted to mean that the maximum compressive horizontal stress vector is NE-SW. The average of the hole elongation azimuths is N35W-S35E. This indicates that the maximum compressive stress vector is N55E-S55W. The acoustic anisotropy vector of N83E-S83W from well B-18 compares with the major stress vector of N60E-S60W from the hole elongation (fig. 27). This 23° disagreement is not insignificant but may be within usable tolerances. The variations between azimuths of the hole

44
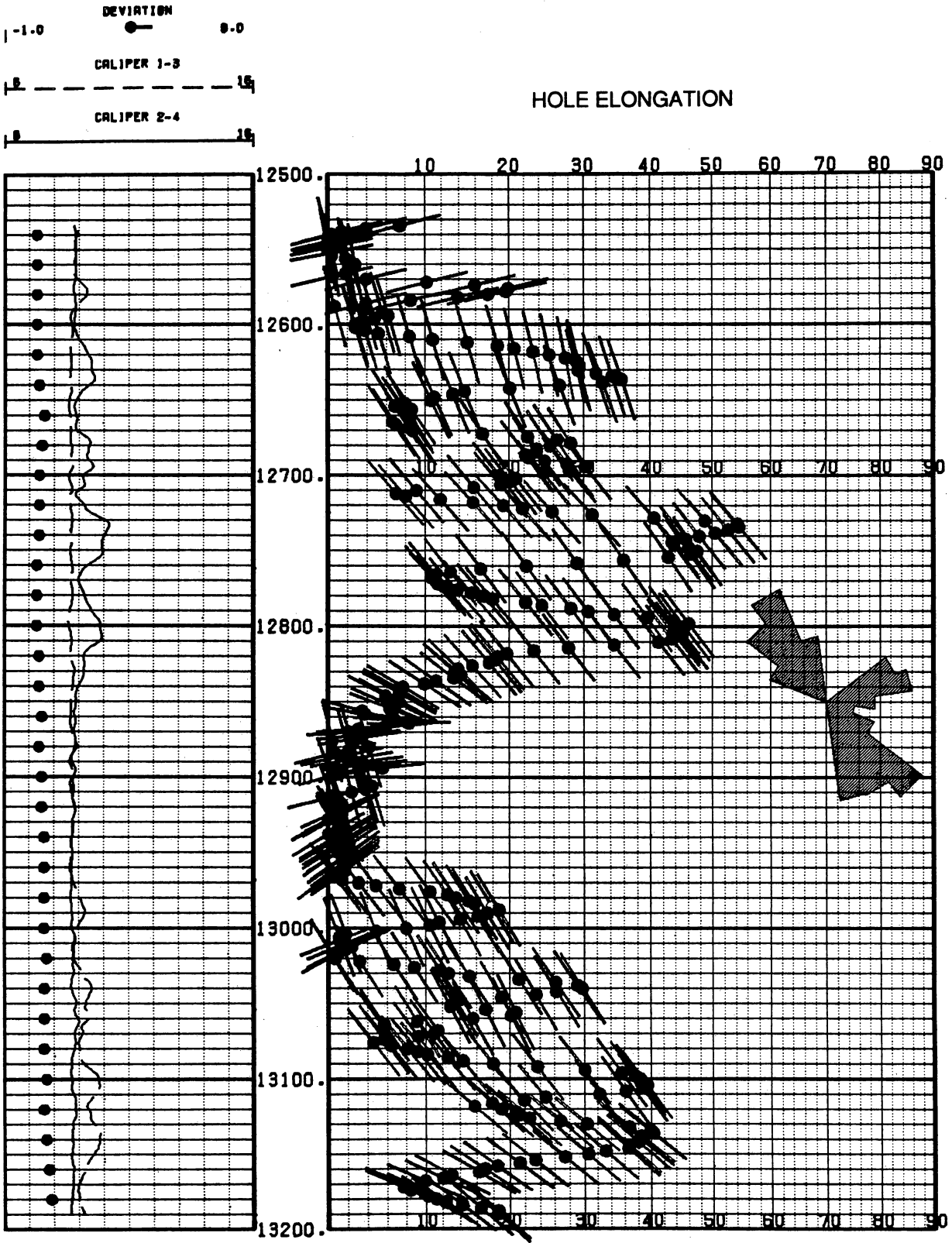
Figure 25. Magnitude and orientation of borehole elongation in the "S" zone, well B-16.
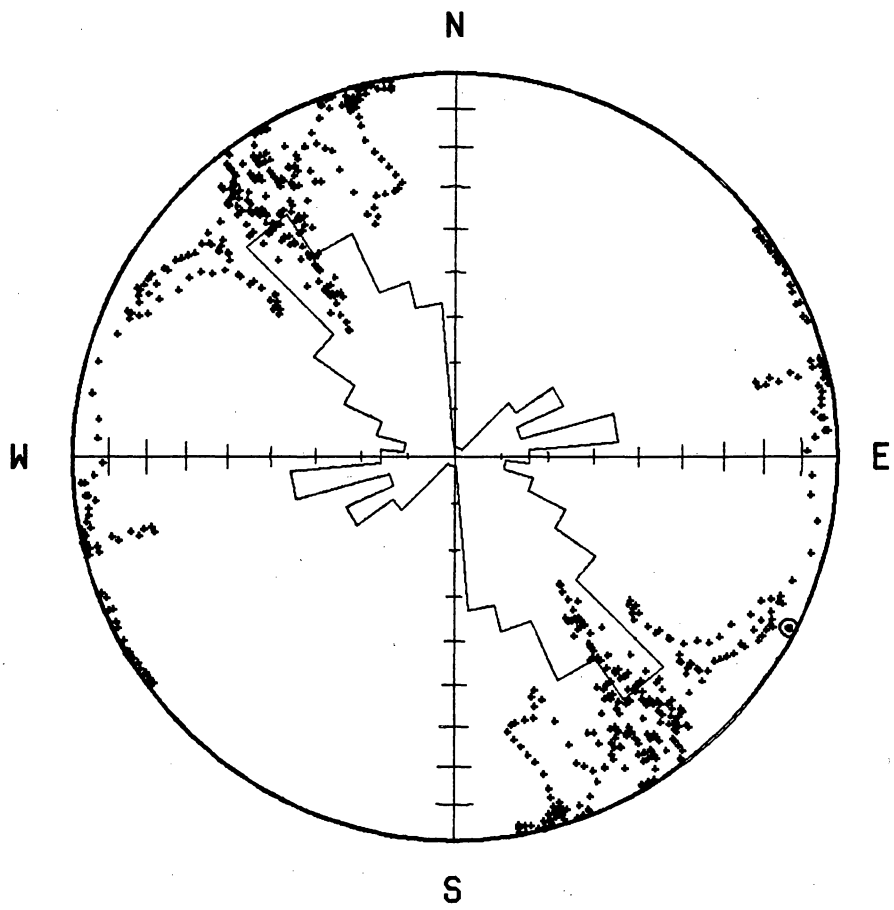
Figure 26. "Propeller plot" of borehole elongations in the "S" zone, well B-16.
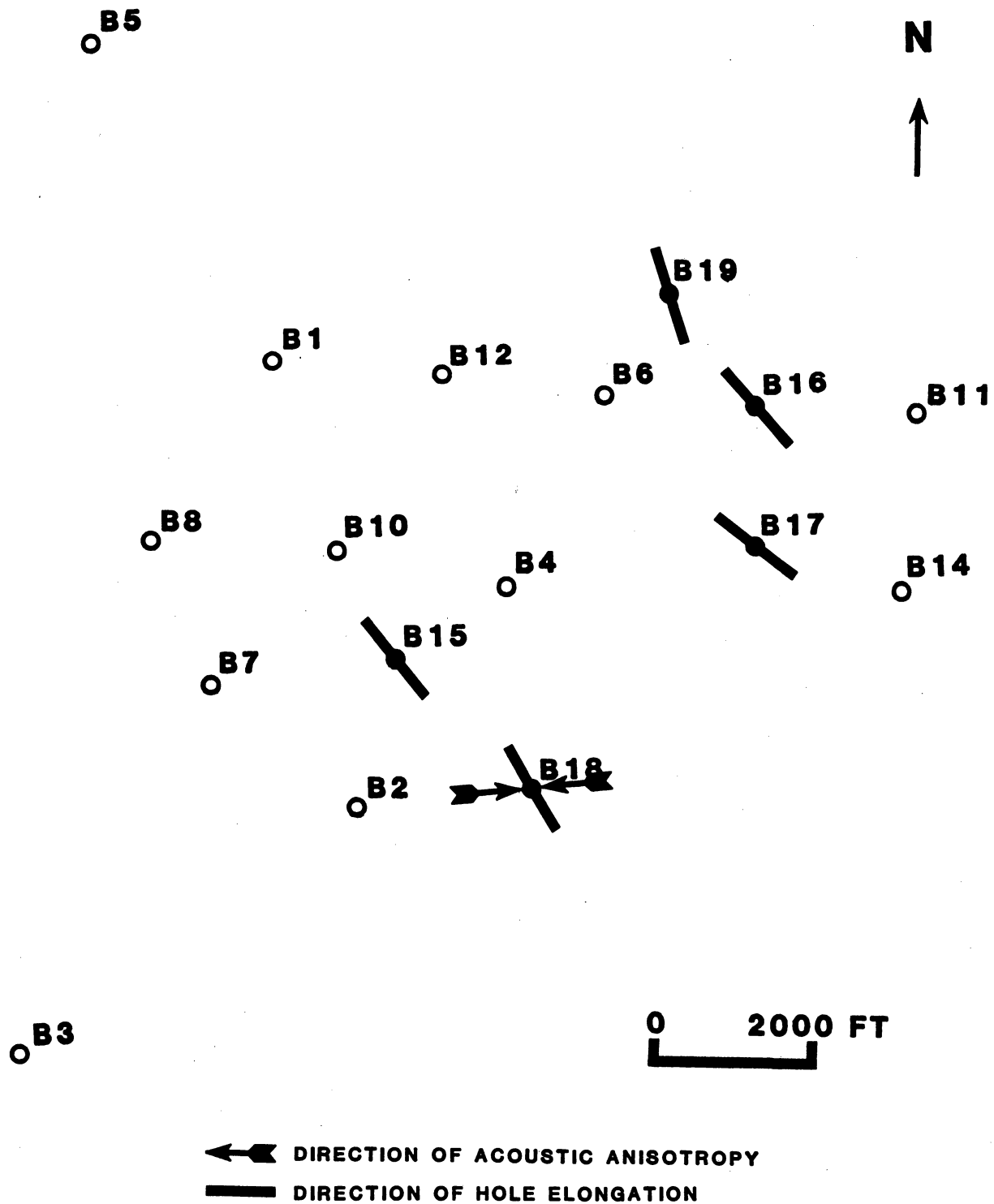
Figure 27. Azimuths of borehole elongation axes and the acoustic anisotropy azimuth.

Table 3. Azimuths of hole elongation.

Well name	Azimuth
B-15	N40W-S40E
B-16	N38W-S38E
B-17	N50W-S50E
B-18	N30W-S30E
B-19	N20W-S20E
Average azimuth	N35W-S35E
Acoustic anisotropy	N83E-S83W

elongation data from well to well are coherent with the changes in dip on the top of the S zone indicated by dipmeters . The northeast wells have a more NW-SE azimuth, whereas the southwest wells have a more WNW-ESE azimuth.

SUMMARY OF RESULTS

The integration of dipmeter data with other data types improves the definition of lateral and vertical changes in reservoirs. The database used for this study consisted of dipmeters and other logs from 15 wells from the Shell McAllen "B" lease in Hidalgo County, Texas. A total of 58,610 ft (17,864.3 m) of dipmeter data was studied. All wells were processed for structural dip data, and five wells, including two with cores, were processed for stratigraphic dip data. Comparison with the cores allowed classical dipmeter interpretation techniques to be adapted to this particular problem.

Rotation of strata into a major growth fault WNW of the B area is the predominant influence on all dipmeters. The sediments affected by the growth fault can be divided into stratigraphically defined domains, rotated to similar dips and azimuths. The variation in azimuths of rotation indicates that the area of maximum subsidence shifted along the axis of the growth fault. Since, in a growth fault zone, the area of maximum subsidence corresponds to the area of maximum deposition, and thus the thickest reservoir sandstones, the inferences drawn from the azimuths of rotation can be used to infer the direction of offset sandstone thicks. This technique successfully predicts the thickness patterns within the S_1 and S_2 sandstones of the Vicksburg S reservoir.

Growth faults may be located by dipmeters through identification of wells with dipmeters exhibiting axes of rotation that differ from the rotations in offset wells. This technique successfully located a growth fault subsequently imaged on recently published three-dimensional seismic data (Hill and others, 1991) between the B-3 well and the rest of the B area wells.

Changes in the number and character of dip domains within the growth fault-influenced section may be used to infer that intervals are not stratigraphically correlative. This technique allows correct interpretation of stratigraphic change rather than faulting of the S reservoir along the western margin of the B area. A similar reinterpretation by Shell Western E & P resulted in 100 Bcf of added reserves since 1987 (Hill and others, 1991).

51

The intervals between dip domains, which mark fault movement, are located at the bases of progradational intervals along strata interpreted to be transgressive shales. Each dip domain represents the progradation of one or more deltaic sandstone.

All wells also contain numerous small "slump patterns" throughout the interval of the growth fault, which may reflect the influence of the growth fault on the local paleoslope because the depositional surface was rotated into the fault (Straccia, 1981). These patterns indicate down-to-the-west rotation, into the growth fault. It is not possible from the dipmeter data alone to distinguish between faults and slumps. If the soft-sediment deformation in fact represents slumps, the slumping will reduce the permeability of the reservoir parallel to the direction of movement and it provides an additional potential source of reservoir heterogeneity that must be considered when locating additional resources within similar gas fields. Although the degree to which slumps restrict the flow of gas cannot be quantified, it provides one possible explanation for the permeability barriers that have been interpreted to exist between S reservoir completions in the B area (Langford and others, in press).

The four-arm oriented calipers from the dipmeters were used to quantify and orient hole eccentricity for comparison with laboratory core measurements of acoustic anisotropy. This comparison indicates that hole eccentricity can be used to predict horizontal stress vectors. These results proved extremely useful in creating a reservoir model of part of the S reservoir in the B area useful to quantify permeability barriers and to identify areas containing potentially unrecovered resources (Langford and others, in press).

APPENDIX A. INDIVIDUAL WELL INTERPRETATIONS-STRUCTURAL.

WELL B-3

The dipmeter log is available over the interval from 10,900 to 15,100 ft (3,322.3 to 4,602.5 m). The dipmeter shows increasing dip associated with rotation on the growth fault toward the northwest over the lower half of this section. The upper half has few changes, with the dips being about 10° toward the north and northeast. This well contains numerous sandstones from 13,290 to 15,100 ft (4,050.8 to 4,602.5 m).

The pattern of increasing dip with depth extends from 12,990 to 15,100 (3,959.3 to 4,602.5 m). At 12,990 ft (3,959.3 m) the strata dip at 12° at 315° azimuth, increasing at 15,100 ft (4,602.5 m) to 40°+ at 305° azimuth. This pattern is due to the growth fault that lies below this well. Throughout this interval there are numerous deflections indicating rotation down to the southeast. Possibly this is due to slump movement toward the northwest. This interval has numerous sandstones and shaly sandstones from 15,100 to 13,280 ft (4,602.5 to 4,407.7 m) at the top of the "S" zone. The interval over which this thick pattern occurs is predicted to thicken to the northwest in the direction of the dip azimuths.

At 12,990 ft (3,959.3 m) the dip azimuths change abruptly toward the north. This marks a change from westward rotation on the growth fault to northward rotation. The dips from 12,990 to 12,520 ft (3,959.3 to 3,816.1 m) appear to have been deposited in a lower energy environment with only minor changes. There are some sandstones in this interval, but they appear to be shaly. At 12,520 ft (3,816.1 m) there is a slight change in the dip azimuths to about N30E, accompanied by an increase in the depositional energy. This interval also becomes sandier toward the top. At 12,040 ft (3,669.8 m) there is an abrupt change to a lower energy, although the dip azimuths are still N30E. The dip magnitudes gradually increase from about 8° at 12,040 ft (3,669.8 m) to about 10° at 11,610 ft (3,538.7

m) with the azimuths remaining about N30E. At 11,610 ft (3,538.7 m) the azimuths abruptly change to about N45E. From 11,610 to 11,175 ft (3,538.7 to 3,406.1 m) the azimuths rotate slowly to about N65E. From 11,175 to 11,050 ft (3,406.1 to 3,368.0 m) there is a pattern where the dips gradually increase from 10° to about 15° and then gradually decrease to 10° at 10,900 ft (3,322.3 m) while the dip azimuths change from N65E to N75E and back to N65E.

WELL B-4

The dipmeter log on this well was available from 11,100 to 14,910 ft (3,383.2 to 4,544.6 m) except for several thick gaps. These gaps are: 14,525 to 14,625 ft (4,427.2 to 4,457.7 m), 13,800 to 14,140 ft (4,206.2 to 4,309.9 m), and 13,400 to 13,450 ft (4,084.3 to 4,099.6 m). These data do not obviously obscure intervals where significant changes occur unless faults happen to be included within these intervals.

The lower portion of this well (12,650 to 14,910 ft [3,855.7 to 4,544.6 m]) displays the increasing dip with increasing depth pattern that is interpreted to be caused by rotation on the growth fault. The dip magnitude decreases from 38° at 14,910 ft (4,544.6 m) to 0° at 12,650 ft (3,855.7 m). The dip azimuth stays close to 310° with no significant change. Above 12,650 ft (3,855.7 m) the dip azimuths change to north and slightly east of north. There is a possible fault at 12,300 ft (3,749.0 m) that is interpreted down to the N55E and striking N35W-S35E. Above this fault to 11,980 ft (3,651.5 m) the dip azimuths are northwest and NNW. At 11,980 ft (3,651.5 m) the dip magnitudes go to near 0°, and above 11,980 ft (3,651.5 m) the dip azimuths are SSW to 11,450 ft (3,490.0 m), where the azimuths rotate to almost due south. The dip patterns from 11,980 to 11,450 ft (3,651.5 to 3,490.0 m) are interpreted to be slump rotation toward the SSW. From 11,450 to 11,100 ft (3,490.0 to 3,383.3 m) the dip patterns are interpreted to be slump rotations toward the south.

The depth 12,650 ft (3,855.7 m) may mark the point where the growth fault ceased to grow or at least ceased to be a significant factor in the deposition of the sediments in this well.

At the top of the S zone at 12,880 ft (3,925.8 m), there is a sharp decrease in the dip magnitude from 10° to 6°. This may indicate an angular unconformity. The sandstones within the S zone all show a similar dip pattern. This pattern is one of increasing dip with depth over the sandstone interval. The shales between the sandstones show very little change of dip with depth. The main sandstone and shale intervals and the dip magnitudes are:

	Interval (ft)	Change in dip magnitude
SAND	13,770-13,800	15° to 26°
SHALE	13,670-13,770	11° to 20°
SAND	13,605-13,670	8° to 22°
SHALE	13,580-13,600	11° to 19°
SAND	13,515-13,580	8° to 22°
SHALE	13,425-13,515	5° to 6°
SAND	13,245-13,425	4° to 27°
SHALE	13,190-13,245	6° to 10°
SAND	13,100-13,190	8° to 24°
SHALE	12,965-13,100	8° to 11°
SAND	12,880-12,965	5° to 15°

WELL B-6

This dipmeter covers the interval from 11,100 to 13,850 ft (3,383.3 to 4,221.5 m). The pattern of increasing dip with increasing depth covers the interval from about 12,600 to 13,850 ft (3,840.5 to 4,221.5 m). The dips increase from 0° at 12,600 ft (3,840.5 m) to 20° at 13,850 ft (4,221.5 m). A possible fault pattern exists at the bottom of the dipmeter interval from 13,700 to 13,850 ft (4,175.8 to 4,221.5 m). The main effects may lie below the dipmeter interval. If this is a fault, the fault plane is inferred to strike N30E-S30W and is downthrown to the ESE. The other major pattern in this interval is from 12,950 to 13,000 ft (3,947.2 to 3,962.4 m) where the dip magnitude changes rapidly from 12° to about 4°. The interval from 12,950 up to 12,600 ft (3,947.2 to 3,840.5 m) shows very little influence of

the growth fault. The interval from 13,000 to 13,850 ft (3,962.4 to 4,221.5 m) shows several short intervals exhibiting rotation, interpreted to be due to slump rotation.

The interval from 11,200 to 12,600 ft (3,413.8 to 3,840.5 m) has low dip magnitude, usually less than 4°, with the dip azimuth mainly eastward at the lower part of the interval and changing to southward at the top of the interval. There is no pattern associated with the dip magnitude.

WELL B-7

The dipmeter interval is from 10,700 to 14,100 ft (3,261.4 to 4,297.7 m). The pattern of increasing dip with increasing depth is from about 11,600 to 14,100 ft (3,535.7 to 4,297.7 m). The dip magnitude decreases from 23° at 14,100 ft (4,297.7 m) to 2° at 11,600 ft (3,535.7 m). The dip azimuth changes from 270° at 14,100 ft (4,297.7 m) to 320° at 11,600 ft (3535.7 m). At the bottom of the interval across a thick sandstone interval, from 13,750 to 14,100 ft (4,191.0 to 4,297.7 m), is a series of dips with magnitudes varying from 15° to 27°. The azimuth of these dips varies from 270° at 14,100 ft (4,297.7 m) to 300° at 13,750 ft (4,191.0 m). At 13,750 ft (4,191.0 m) the dip suddenly reduces from about 22° to 15°. The azimuth stays at about 300°. This point marks a depositional break during which the growth fault moved. Over the interval from 13,410 to 13,750 ft (4,087.4 to 4,191.0 m), dip increases more slowly with increasing depth. Dip magnitude increases from about 12° at 13,410 ft (4,087.4 m) to 15° at 13,750 ft (4,191.0 m). This could have been caused by slow and gradual rotation by the growth fault.

The next pattern occurs from 13,125 to 13,410 ft (4,000.5 to 4,087.4 m) and appears to be a long gentle slump pattern with three or four smaller patterns occurring within the thicker pattern.

From 12,880 to 13,125 ft (3,925.8 to 4,000.5 m) is another thick slump pattern that at the bottom shows some azimuth change toward the north. The azimuth at 13,125 ft (4000.5 m) is 300°, whereas the azimuth at 12,880 ft (3,925.8 m) is 280°.

The interval from 11,600 to 12,880 ft (3,535.7 to 3,925.8 m) appears to be the top of the interval rotated by the growth fault. There is a gradual decrease in magnitude as you come up the hole.

56

At 12,880 ft (3,925.8 m) the magnitude is 8°, which reduces to 1° at 11,600 ft (3,535.7 m). There is no significant dip azimuth change over this interval.

From 11,600 to 11,400 ft (3,535.7 to 3,474.7 m) the dips are about 1° to 2° magnitude, but the azimuth rotates from northeast to north to east. Starting at 11,400 ft (3,474.7 m) the dips increase in magnitude to about 4°, with the azimuth being due east to 11,080 ft (3,377.1 m). At 10,800 ft (3,291.8 m) the azimuths suddenly change to SSE and southeast up to 10,700 ft (3,261.4 m).

WELL B-8

The dipmeter covers the interval from 11,500 to 15,000 ft (3,505.2 to 4,572.0 m). The increasing dip magnitude with increasing depth pattern covers the interval from 11,700 to 15,000 ft (3,566.2 to 4,572.0 m). This is a very long interval, and it is possible that the growth fault rotation may end at about 13,000 ft (3,962.4 m). However, the sediments from 11,500 to 13,000 ft (3,505.2 to 3,962.4 m) appear coherent with the sediments below 13,000 ft (3,962.4 m), as there is no significant discontinuity. There is an abrupt change in dip magnitude from about 7° at 13,800 ft (4,206.2 m) to about 23° at 14,100 ft (4,297.7 m). If this pattern was caused by rotation by the growth fault, it indicates that most of the movement occurred while this interval was being deposited. An alternate interpretation would be that there is another fault at 14,000 ft (4,267.2 m) that rotated the sediments below 14,000 ft (4,267.2 m) and deformed the sediments from 13,800 to 14,000 ft (4,206.2 to 4,267.2 m) into the fault plane. Below 14,000 ft (4,267.2 m) there are several thick patterns. The dips from 14,775 to 15,000 ft (4,503.4 to 4,572.0 m) average higher than the dips above. The next coherent interval is from 14,330 to 14,775 ft (4,376.8 to 4,503.4 m). There is indication of rotation by a possible fault or slump at 14,660 ft (4,503.4 m). This interval is mostly sandstone with several small shale breaks. The dip increases from 22° at 14,360 ft (4,377.0 m) to 25° at 14,750 ft (4,495.8 m). This small increase indicates that little rotation occurred while this interval was being deposited. The next coherent interval is from 14,055 to 14,330 ft (4,284.0 to 4,367.8 m). The dips indicate significant movement of the growth fault at 14,330 ft

(4,367.8 m). There is a small pattern at 14,270 ft (4,349.5 m) that could indicate rotation on a small fault or slump.

The interval from 13,790 to 14,055 ft (4,203.2 to 4,284.0 m) reflects the major rotation on the growth fault. The dips at 14,055 ft (4,284.0 m) are 25° compared to dips of 6° at 13,790 ft (4,203.2 m). There is a short interval of fault or slump rotation at 14,000 ft (4,267.2 m). This depth also marks the base of an upward-coarsening sandstone.

The next coherent interval is from 13,150 to 13,790 ft (4,008.1 to 4,203.2 m). This interval appears to have been deposited in a low-energy environment with little movement of the fault. There are some short rotational patterns at 13,550, 13,350 and 13,175 ft (4,130.0, 4,069.1, and 4,015.7 m), which could be small faults or slumps, but they do not appear to have significantly altered the depositional cycle.

The interval from 13,070 to 13,150 ft (3,983.7 to 4,008.1 m) covers a change in dip magnitude from 7° at the bottom to 3° at the top. This is interpreted as being a period when beds were rotated rapidly on the fault. The top of this interval marks the base of a series of three sandstones which all appear to be upward coarsening.

The interval from 12,240 to 13,070 ft (3,730.7 to 3,983.7 m) appears to be a period of no or little movement of the growth fault. There is another sandstone from 12,330 to 12,500 ft (3,758.2 to 3,810.0 m), near the top of the interval, which also seems to be upward cleaning. The patterns at 12,940, 12,850 and 12,500 ft (3,944.1, 3,916.7, and 3,810.0 m) appear to be small slump rotations.

The interval 11,500 to 12,240 ft (3,505.3 to 3,730.7 m) appears to have been deposited during a period of steady rotation on the growth fault. The dip at the bottom of the interval is 3°, which gradually decreases to 1.5° at the top of the interval.

The patterns and identifiable intervals in this well indicate that this fault moved in several stages followed by periods of very little movement. These patterns are not as evident in wells farther away from the fault because rotation is more poorly defined. The wells farther away display patterns that indicate more continuous movement of the fault.

58

WELL B-10

The dipmeter is available from 10,700 to 13,800 ft (3,261.4 to 4,206.2 m). The increasing dip with increasing depth pattern occurs from 13,170 to 13,800 ft (4,014.2 to 4,206.2 m). The dip magnitude increases from 0° at 13,170 ft (4,014.2 m) to 17° at 13,800 ft (4,206.2 m), with a possible fault or slump rotation from 13,500 to 13,550 ft (4,114.8 to 4,130.0 m). There is a change in azimuth toward the north toward the top of the pattern, indicating that the interval was tilted north or northeast after deposition.

The interval from 12,280 to 13,170 ft (3,742.9 to 4,014.2 m) has coherent dips. There are short intervals with rotation toward the southwest and SSW, suggesting slumps toward the northeast along with possible soft-sediment deformation and possible faults. There is indication of a small fault at 12,550 ft (3,825.2 m) striking N-S and downthrown to the east. There is a smaller fault indicated at 12,810 ft (3,904.5 m) striking NE-SW and downthrown to the southeast. The dips in this interval are to the south. The average dip magnitude increases from 13,170 ft (4,014.2 m) up to the possible fault at 12,550 ft (3,825.2 m). Above the fault, dips decrease up to 12,280 ft (3,742.9 m). This interval contains two shaly sandstones.

The interval from 12,020 to 12,280 ft (3,261.4 to 3,663.7 m) has dips that rotate between northeast and southwest in azimuth. At the top of the interval the dip magnitude goes to near 0°.

The interval from 10,700 to 12,020 ft (3,261.4 to 3,663.7 m) appears to contain mostly silty shale with two very shaly sandstones. The dip magnitude varies from 4° at 11,800 ft (3,596.6 m) to 8° at 11,200 ft (3,413.8 m) back to 6° at 10,700 ft (3,261.4 m). The dip azimuth varies from 135° at 11,800 ft (3,596.6 m) to 125° at 11,200 ft (3,413.8 m) to 180° at 10,700 ft (3,261.4 m). This interval is interpreted as gradually tilting southward during deposition.

WELL B-11

The dipmeter covers the interval from 10,600 to 13,740 ft (3,230.9 to 4,187.9 m). The increasing dip with increasing depth pattern covers the interval from 11,550 to 13,740 ft (3,520.4 to

4,187.9 m). This dips show a gradual rotation toward the northeast as you move from the bottom to the top. This rotation would have been caused by a 5° rotation toward N45E. This pattern shows several intervals where the rotation into the fault appears to have slowed or stopped. The interval from 13,600 to 13,740 ft (4,145.3 to 4,187.9 m) contains three thick slump or fault patterns down toward N60W. These are most likely oriented toward the major movement of the growth fault. The interval from 13,400 to 13,600 ft (4,084.3 to 4,145.3 m) was most likely deposited during a period of little fault movement. The interval from 13,050 to 13,400 ft (3,977.6 to 4,084.3 m) appears to have been deposited during a period of greater movement. The interval from 12,800 to 13,050 ft (3,901.4 to 3,977.6 m) seems to have been deposited during a period when the movement of the fault was minor. The interval from 12,600 to 12,800 ft (3,840.5 to 3,901.4 m) indicates more rapid movement of the fault. The interval from 12,350 to 12,600 ft (3,764.3 to 3,840.5 m) is another period of little apparent movement of the fault, although there are patterns that indicate slumps or faults into the growth fault. The interval from 12,180 to 12,350 ft (3,712.5 to 3,764.3 m) indicates more movement of the fault during deposition. The interval from 11,675 to 12,180 ft (3,558.5 to 3,712.5 m) suggests little movement of the fault during deposition. The interval from 11,550 to 11,675 ft (3,520.4 to 3,712.5 m) indicates more movement of the fault. There is rotation interpreted as a slump or fault pattern at 11,660 ft (3,554.0 m) toward the growth fault.

WELL B-12

The dipmeter covers the interval from 11,100 to 14,440 ft (3,383.3 to 4,401.3 m). The increasing dip with increasing depth pattern covers the interval from 12,800 to 14,440 ft (3,901.4 to 4,401.3 m). The dips increase from near 0° at 12,800 ft (3,901.4 m) to 22 ° at 14,440 ft (4,401.3 m). This pattern can be divided into several intervals that may reflect the periods of movement or stability of the growth fault. The interval from 14,150 to 14,440 ft (4,312.9 to 4,401.3 m) appears to represent a period when the fault moved very little. The interval from 14,000 to 14,150 ft (4,267.2 to 4,312.9 m) seems to represent a period when the fault was moving. The interval from 13,780 to 14,000 ft (4,200.1

to 4,267.2 m) appears to be a period of little movement of the fault. The interval from 13,740 to 13,780 ft (4,187.9 to 4,200.1 m) seems to represent a period when the fault was active. The interval from 13,390 to 13,740 ft (4,081.3 to 4,187.9 m) appears to represent a period of little movement of the fault. This interval appears to have several slump rotation patterns. The interval 13,250 to 13,390 ft (4,038.6 to 4,081.3 m) seems to be affected by movement of the fault. There is a thick slump or fault rotation at 13,240 to 13,270 ft (4,035.5 to 4,044.7 m). The interval from 13,030 to 13,250 ft (3,971.5 to 4,038.6 m) appears to be another interval when the fault moved very little. The interval from 12,800 to 13,030 ft (3,901.4 to 3,971.5 m) is apparently affected by a thick fault at 12,965 ft (3,951.7 m). This fault strikes E-W and is downthrown to the south. The rotation caused by the growth fault is interpreted to extend through this fault zone to approximately 12,800 ft (3,901.4 m).

The interval from 11,100 to 12,800 ft (3,383.3 to 3,901.4 m) appears to be a coherent depositional interval. This interval has been rotated about 6° toward 160° azimuth. That this occurred without affecting the dip data below 13,000 ft (3,962.4 m) indicates that the rotation was most likely associated with the fault at 12,965 ft (3,951.7 m). This indicates that the fault, which is down to the south, rotated the sediments above the fault. A block rotation is inferred because the sediments at the base of this interval directly above the fault do not appear to have been tilted more than the sediments at the top of the dipmeter interval. When a dip of 6° at 180° azimuth is rotated from this interval, it appears that this interval may have also been deposited under the influence of a growth fault that is located northeast of this well.

WELL B-14

The dipmeter covers the interval from 11,300 to 13,830 ft (3,444.2 to 4,215.4 m). The increasing dip with increasing depth pattern covers the interval from 12,150 to 13,830 ft (3,703.3 to 4,215.4 m). The interval from 12,420 to 13,450 ft (3,785.6 to 4,099.6 m) appears to be a time when the fault moved rapidly. The interval from 13,290 to 12,420 ft (4,050.8 to 3,785.6 m) was a period when the fault was stable. The interval from 13,270 to 13,290 ft (4,044.7 to 4,050.8 m) appears to be a time when

61

the fault moved. The interval from 13,050 to 13,270 ft (3,977.6 to 4,044.7 m) was another stable period. The interval from 12,800 to 13,050 ft (3,901.4 to 3,977.6 m) also was a period when the fault moved. At 12,800 ft (3,901.4 m) the rate of movement appears to increase slightly to 12,580 ft (3,834.4 m). The thick pattern from 12,350 to 12,580 ft (3,764.3 to 3,834.4 m) appears to be a slump pattern or soft-sediment deformation pattern. This interval includes some sandstones that could be caused by sand slumping from a shelf toward the fault. The top of this pattern was extrapolated to 12,150 ft (3,703.3 m). This appears to possibly lap onto the pattern that exists toward the top of the dipmeter section.

From 11,300 to 12,150 ft (3,444.2 to 3,703.3 m) is a pattern of decreasing dip with increasing depth. This pattern changes from 18° to 0° in dip magnitude over this interval, which is a large change in magnitude to be caused by change in structural dip due to a structure that has an inclined axis or is asymmetrical. This pattern also indicates some slumping or faulting down to the south. A valid interpretation of this pattern will require additional information.

WELL B-15

The dipmeter covers the interval from 9,485 to 14,650 ft (2,891.0 to 4,465.3 m). The thick increasing dip with increasing depth pattern extends from 12,300 to 14,650 ft (3,749.0 to 4,465.3 m). The dip increases from 0° at 12,300 ft (3,749.0 m) to 25° at 14,650 ft (4,465.3 m). Within this interval are several smaller patterns indicating rotation on possible slumps at 14,560, 14,300, 14,150, 14,050, 13,830, 13,700 and 13,210 ft (4,437.9, 4,358.6, 4,312.9, 4,282.4, 4,215.4, 4,175.8 and 4,026.4 m). Dip changes from 21° to 25° over the interval from 13,400 to 14,650 ft (4,084.3 to 4,465.3 m). This indicates that the growth fault did not move much during deposition of this interval. The interval from 13,150 to a 13,400 ft (4,008.1 to 4,084.3 m) has a large dip change, which indicates that the fault may have been active during this period of deposition. The interval from 13,000 to 13,150 ft (3,962.4 to 4,008.1 m) appears to be rotation on a fault or slump. The interval from 12,650 to 13,000 ft (3,855.7 to 3,962.4 m) appears to be a fault zone. The fault(s) strike NE-SW and are downthrown to the northeast.

The interval from 12,425 to 12,650 ft (3,787.1 to 3,855.7 m) is an interval of slow movement of the growth fault.

The interval from 9,485 to 11,600 ft (2,891.0 to 3,535.7 m) has a pattern of decreasing dip with increasing depth. This could be interpreted as resulting from several phases of deformation or to an E-W striking fold. At 11,600 ft (3,535.7 m) the well bore would be near the crest of the feature, whereas at 9,485 ft (2,891.0 m) the axis of the feature has moved northward. This pattern is similar to the pattern in the upper portion of well B-14, but the dip magnitude change in this well is much lower.

WELL B-16

The dipmeter covers the interval from 9,050 to 15,000 ft (2,758.4 to 4,572.0 m). The thick increasing dip with increasing depth pattern covers the interval from 11,950 to 15,000 ft (3,642.4 to 4,572.0 m). The dip magnitude varies from near 0° at 11,950 ft (3,642.4 m) to 38° at 15,000 ft (4,572.0 m). The azimuth at 15,000 ft (4,572.0 m) is 300° changing to due north at the top of the pattern. Fault patterns are indicated at 14,420, 14,200, 13,900, 13,600, 13,360 and 13,225 ft (4,395.2, 4,328.2, 4,236.7, 4,145.3, 4,072.1, and 4,031.0 m). The faults appear to be down to the west and to strike N-S. The pattern of increasing dip associated with the growth fault shows a swing in azimuth toward the northeast at the top.

The interval from 9,050 to 11,950 ft (2,758.4 to 3,642.4 m) shows westward dip, gradually decreasing from 9° at 9,050 ft (2,758.4 m) to 1° at 11,950 ft (3,642.4 m). Fault patterns are indicated at 10,200, 10,000 and 9,540 ft (3,109.0, 3,048.0, and 2,907.8 m). These faults are down to the west. The dip azimuths vary between slightly north of west to slightly south of west.

WELL B-17

The dipmeter interval is from 9,020 to 14,280 ft (2,749.3 to 4,352.5 m). The growth fault pattern extends from 11,625 ft (3,543.3 m) to TD. The dips change from 28° at TD to 0° at 11,625 ft

(3,543.3 m). The dips rotate toward the northeast at the upper portion of the pattern. This indicates that the entire interval of this pattern was rotated down to the northeast. There is a thick interval showing slump rotation from 13,725 to 13,975 ft (4,183.4 to 4,259.6 m). Dip magnitude reduces from 23° to 18° across this slump. Another slump pattern extends from 13,390 to 13,425 ft (4,081.3 to 4,091.9 m). This second pattern also marks a sudden change in the dip magnitude of the growth fault pattern. This sudden change from 20° to 8° is probably due to rapid movement of the growth fault over this interval. From 13,390 to 11,625 ft (4,081.3 to 3,543.3 m) the dip magnitude changes from 8° to 0°. This gradual reduction in dip indicates the growth fault moved gradually over this interval.

The interval from 9,020 to 11,625 ft (2,749.3 to 3,543.3 m) is a decreasing dip with increasing depth pattern. The dip magnitude at 9,020 ft (2,749.3 m) is 10°, decreasing to 0° at 11,625 ft (3,543.3 m). The dip azimuths change from due south at 9,020 ft (2,749.3 m) to WSW at 11,625 ft (3,543.3 m). There is a thick interval showing rotation interpreted as a fault pattern at 11,000 ft (3,352.8 m). This fault strikes E-W and is downthrown to the south.

WELL B-18

The dipmeter covers the interval from 9,700 to 13,975 ft (2,956.6 to 4,259.6 m). The growth fault pattern extends from 11,850 ft (3,611.9 m) to TD. From 12,810 ft (3,904.5 m) to TD the dip magnitude increases from 7° to 17° and includes several intervals exhibiting slump patterns that tend to correlate with the sandstones. At 12,810 ft (3,904.5 m) the dip magnitude suddenly changes from 7° to 4°. The dip magnitude slowly decreases to 0° at 11,850 ft (3,611.9 m). From 11,850 to 9,700 ft (3,611.9 to 2,956.6 m) the dips are between 0° and 7° toward the SSE. The dip magnitude increases from 0° at 11,850 ft (3,611.9 m) to 7° at 10,850 ft (3,307.1 m), decreasing to 3° at 9,700 ft (2,956.6 m). There is a thick rotated interval interpreted as fault pattern from 10,900 to 11,125 ft (3,322.3 to 3,390.9 m). This fault strikes E-W and is downthrown to the south.

The sandstones in this well occur from 12,810 ft (3,904.5 m) to TD over the interval where the growth fault appears to be most active.

WELL B-19

The dipmeter interval is from 9,775 to 14,060 ft (2,979.4 to 4,285.5 m). The growth fault pattern extends from 12,265 ft (3,738.4 m) to TD. Dip increases in magnitude from 0° at 12,265 ft (3,738.4 m) to 20° at 14,060 ft (4,285.5 m). Included in this interval are several smaller slump patterns that tend to correlate with the sandstones.

The interval from 12,265 to 11,475 ft (3,738.4 to 3,497.6 m) dips southward 3° to 4°. There are small fault patterns at 12,210 and 15,550 ft (3,721.6 and 4,739.6 m). The fault pattern at 12,210 ft (3,721.6 m) strikes E-W and is downthrown to the south. The pattern at 15,550 ft (4,739.6 m) strikes NE-SW and is downthrown to the southeast.

From 11,475 to 9,775 ft (3,497.6 to 2,979.4 m) the dips are southeast at 8° to 10°. Fault patterns exist at 10,475 and 10,175 ft (3,192.8 and 3,101.3 m). Both of these faults strike ENE-WSW and are downthrown to the NNE.

APPENDIX B. DIPMETER PROCESSING--COMPUTATION AND PRESENTATION.

THEORY OF DIP MEASUREMENT AND COMPUTATION

The computation of formation dips from the dipmeter data starts with the correlation between the pad-mounted microresistivity curves. These correlations were originally done by optical comparison of the curves in a manner very much like that of correlating ordinary well logs from well to well. However, instead of being between wells, the correlation is done between pads around the well bore. In the short distance around the well bore, the displacements between curves can be very small, of the order of a few tenths of an inch. The calipers are used to identify exactly how far apart these curves are around the well bore so that a dip plane can be computed that honors the correlations made between the pads. The tool is oriented in the earth's magnetic and gravitational fields so both the azimuth of the dip can be oriented to true north and the magnitude measured from the horizontal (Moran, 1962).

Due to the high density of depth-based data (up to 120 samples per foot of well bore for each pad or electrode), this processing is very machine intensive compared with the processing of other depth-based data in the well. However, the computations do not require as much human intervention as do normal petrophysical computations. The selection of parameters used in the computation can be selected through use of some simple rules or by using the same parameters as were used on the last well. These computation parameters are mainly represented by three numbers. These numbers represent:

> Correlation Length: The length of wellbore micro-resistivity data that is
>
> used to correlate with like lengths of similar data around the well bore.
>
> This length is usually given in feet or meters but can be given in inches or
>
> centimeters. The most common length is 4 ft (1.2 m).

Step Length: The distance between adjacent correlation lengths. Can
be given either as a distance in the same units as the correlation length or
as a percentage of the correlation length. The most common step length
is 2 ft (.6 m) which would be a 50% step using a 4 ft (1.2 m) correlation
length.

Search Angle: The maximum angle away from horizontal that is
attempted to be correlated. Usually given in degrees, although some
companies use a search length that is the distance from horizontal (both
up and down) that the curves are displaced in an effort to identify a
correlation. When a search angle is given in degrees, this angle can be
referenced one of three ways: (1) with respect to the horizon, (2) with
respect to the borehole, and (3) with respect to a structural plane
identified by magnitude and azimuth.

The dip that the program must first locate is the dip with respect to the well bore. If the well bore
is highly deviated and drilling downdip, this apparent dip can be higher than the dip you will want to
measure. This well-bore deviation is added to the expected structural dip before the true dip can be
determined.

The correlations between curves are effected by comparing mathematical relationships
between any two curves at each correlation step up and down the well bore. These mathematical
relationships assume many forms and are referred to as "correlation algorithms." Many are similar to the
algorithms used in seismic processing. Once these correlation displacements are computed, a plane is
computed that passes through the points that mark the displacements. The dip of this plane is apparent
dip because it is computed with respect to the well bore. The tool navigation data are then used to
correct for the deviation of the well bore. The result is the computed dip with respect to the horizontal.

The dip computed from these data is somewhat an average of the bedding dips that exist in the
correlation interval. This means that longer correlation lengths average numerous beds and thus reflect
structure. Shorter correlation lengths average fewer beds and thus tend to reflect variation between

different beds and more depositional information. "Longer" and "shorter" are in relationship to the thickness of the genetic depositional units. In shales this thickness may be of the order of tenths of an inch, whereas in eolian deposits it may be several tens or even several hundreds of feet.

By using a correlation step that is less than the correlation length, there is less chance of missing a valid correlation feature because the feature is divided between two of the correlation lengths. But this can also repeat computed dips if the same strong resistivity feature overlaps two adjacent computations. However, this can usually be recognized and allowance made in the interpretation.

The search angle chosen must obviously be high enough to find the existing dips. However, if the angle is extraneously high, two adverse effects are noted. The first is a disproportionate increase in machine computation time as the angle is increased, because the machine time increases linearly as the distance up and down the well bore increases. This distance is a function of the tangent of the search angle with respect to the well bore. The tangent changes from 0 at 0° search angle to an infinitely large number at 90° search angle. Therefore it is prudent to select an angle that is equal to or only slightly larger than the maximum angle you expect to find. The other adverse effect is that as the search angle is increased, the likelihood of finding a random correlation increases. This likelihood also increases directly as the tangent increases, causing the random dips to increase as you near the search angle limit.

In everyday practice, correlation lengths vary from 4 ft (1.2 m) for most water-based mud applications to 8 ft (2.4 m) for most oil-based mud applications when searching for structural dips. But it is possible to extend correlation lengths up to 20 ft (6.1 m) or more if attempting to define low or subtle structural dip. For stratigraphic or sedimentary interpretations, correlation lengths may be as low as 1 to 2 inches (2.5 - 5 cm) to 1 to 2 ft (.3 - .6 m). Examination of the resistivity curves can be an aid in determining an optimum length where most sedimentary features are described on the resistivity curves.

Some other variables in the selection of processing parameters are well-bore condition, well-bore fluid, tool design, tool condition, formation characteristics, and acquisition techniques. Careful selection of the computation parameters is important to the resultant computed dips, and it is only when all variables are optimized that the best formation dip data can be retrieved.

69

ADDITIONAL COMPUTATIONS AND PROCESSING

Other processing options, such as dip subtraction, dip projection, result filtering, dip vector addition, and conversion from depth-based data to time-based data, are available to aid the dipmeter interpretation. These processings can be aids to the interpretation and the integration of dipmeter data into other data sets.

PRESENTATIONS OF DIPMETER DATA

The usual presentation of a dip datum is as a "dip tadpole." The center or body of the tadpole identifies the depth (or time) of the computed dip and the magnitude of the computed dip. The azimuth of the computed dip is reflected by the direction of the tail of the tadpole, with the convention being that the top of the log is north. The quality of the computed dip is often displayed by the coding of the tadpole body. This presentation can be made on any depth scale and can include other data such as calipers, hole deviation, and other logs for correlation.

Other depth-based (or time-based) presentations include separated plots, where the dip magnitude and the dip azimuth are plotted separately as points or curves, cylinder plots, and stick plots, where the dip magnitudes are projected along specified azimuths.

Other presentations include Schmidt and Wulff plots of vectors or poles, tangent plots, histograms, dip versus azimuth crossplots, tabular listings of dip results, and azimuth vector plots.

Because the dipmeter has multiple calipers and must record tool navigation information, other supplemental data become available. These include oriented calipers, hole deviation surveys, and hole volume for cement estimation.

The oriented calipers are useful in describing and orienting the geometry hole. This can aid in selecting packer points or any other activity that depends on the configuration and orientation of the hole.

APPENDIX C.   INTERPRETATION THEORY.

GENERAL BASIS FOR DIPMETER INTERPRETATION

Since most deposition occurs on a nearly horizontal surface, we can presume that the original formation dip was near 0°. And since the physical and electrical characteristics of the sediments are much more likely to be similar parallel to the surface of deposition than at some angle to this surface, we can define this surface by correlation of the electrical or physical parameters along these surfaces. We use this same principle when we make well-to-well correlations with electric logs. In the case of the dipmeter we are making these correlations around a well bore. This allows the dipmeter to reflect the present-day attitude of the surface of deposition, which may have been altered by tilting or deformation.

The dip of the original surface of deposition usually reflects either the local slope of the depositional surface (controlled by gravity) or the dip of foresets or other small-scale depositional features of the sediments. Most dipmeter computed dips reflect the local paleoslope, which usually closely reflects the structural dip. Since dips that reflect transport direction usually occur within sedimentary units with boundaries that reflect the local paleoslope, the longer correlation lengths tend to reflect structural dips while the shorter correlation lengths will have more dips that reflect interval features. As these dips are altered by faulting, tilting, or folding, we get altered data that can then be interpreted in a geological context.

Before dipmeter interpretation begins, the interpreter must have knowledge of the geological setting of the area. Growth faults, turbidites, normal faults, reverse faults, reefs, overthrusts, deltas, draping, slumps, stream channels, beaches, etc., all have different geological characteristics that must be understood before they can be interpreted. The dipmeter can give only a limited amount of data to reconstruct these widely varying cases (Campbell, 1968; Gilreath and Maricelli, 1964). It will obviously

not be possible to define all these situations from dipmeter data only, but the dipmeter can offer clues as to the following:

1. Local paleoslope direction: Since most sediments thicken downslope, and most linear depositional units trend perpendicular to the local paleoslope, this information can be very important to the mapping or the location of offset wells. This will also aid in identifying the structural position of offset wells when the structural dip is very low.

2. Transport direction: This will be perpendicular to the local paleoslope in cases such as fluvial deposits and parallel to the local paleoslope in cases such as beach or bar-type deposits.

3. Thickness of sedimentary features: These can range from less than a tenth of an inch to several hundred feet. This determination of thickness can aid in defining the particular environment as well as the energy of the environment.

Because the dipmeter measurements are of necessity confined to and near the well bore, the computed dips do not correlate directly with dip data taken from seismic or well-to-well correlations. This is because the dipmeter gathers dip data that has limited horizontal dimensions but extensive vertical dimensions. Usually dip information from outcrops or subsurface geology is gathered in a lateral or horizontal dimension. Translation of horizontal information into the vertical dimension is a routine step in geology. The dipmeter acquires dip data in the vertical dimension, which must then be translated to the horizontal dimension. If the dipmeter reflects a dip pattern over 1000 to 2000 ft (304.8 to 609.6 m) of interval, it is likely that this feature has significant lateral extent. Conversely, if the pattern is reflected only over 5 ft (1.5 m) of hole with nothing above or below the feature to reinforce it, the feature probably does not extend very far laterally.

In areas where structural dip is low and subsurface control is sparse, the dipmeter can be used in combination with subsurface data to identify anomalies that may not be evident from either data set alone. In many cases, the transport direction and local paleoslope can be interpreted.

Fault location and orientation are two of the oldest uses of dipmeters. The presence of a fault must usually be determined by well-to-well correlations, as dipmeter fault patterns can be ambiguous. The dipmeter is unable to detect the fault plane itself, but it will respond to the bed deformation associated with the faulting. By examining this bed deformation, the location, strike, and upthrown/downthrown blocks can be identified. The bed dips at the point of maximum bed deformation can indicate a minimum dip angle for the fault plane. It is not usually possible to differentiate between normal and thrust faults, so this also must be done with subsurface geology. Careful examination of the dip azimuths above and below the fault can indicate the presence of any rotation across the fault. This can help describe the type of fault or be a clue as to the nearest direction in which the fault will die out.

Dip data from the dipmeter lend themselves well to special plots, both to summarize the statistical type of data obtained by making correlations every few feet (and in some cases every few inches) of well bore and to discern subtle changes in dip magnitude and dip azimuth over several hundreds or thousands of feet.

STRUCTURAL INTERPRETATION

Structural dips are computed when the correlation length is several times the thickness of the genetic sedimentary units. Four feet (1.2 m) is the most commonly used length to use for structural computations, although lengths of 8 ft and 12 ft (2.4 - 3.7 m) are not uncommon. If it is known that the sediments are such that bedding over a 4 ft (1.2 m) interval is not representative of the structural dips, then a longer length must be used for the computed dips. This might be the case in some eolian deposits. In these cases it may become necessary to examine the dipmeter results at particular points or intervals that have been identified as reflecting structure.

Structural dip is defined as dip created by deformation of the rock. This information can usually be projected laterally a significant distance-to an offset well in most cases. Because the dip computed from a dipmeter is done from points only a few inches apart on beds, it is important that small local variations be minimized when attempting to measure structural dip at the boundary with a dipmeter. By

73

using a vertical interval of 4 to 8 ft (1.2 - 2.4 m) for the correlation, some averaging is done in the dip computation. However, it is usually necessary to examine dip data over some vertical interval to identify the average. The identification of the location and length of this particular vertical interval, which can be used to describe the structural dip, is an interpretation. The first place to look for such an interval is at or directly above the boundary you are attempting to map. However, it is sometimes necessary to look some distance above the boundary before the data reflects the dip that exists between wells and not the dip that exists locally on the surface of the boundary. This exercise can be compared with that of identifying a shallow horizon, which, when mapped, reflects the surface of a deeper horizon.

The important relationship is that the longer the vertical well-bore distance that reflects a coherent dip value, the greater the horizontal distance that this dip can be extrapolated. This relationship starts with the correlation length that is used to compute a dip and extends to the interpretation of the structural dip from the dipmeter.

STRATIGRAPHIC INTERPRETATION

The use of the dipmeter to identify the dips associated with local paleoslope and transport direction requires more interpretation than the identification of structural dip. The process begins with the selection of the correlation length. This length should be equal to or less than the thickness of most features that are expected. In low-energy depositional environments, where beds are often thin, this may be 1 to 2 in (2.5-5 cm). In higher energy environments, where cross strata are common features and beds are thicker, it may be 6 to 12 in (15-30 cm). The quality of the raw acquisition data also will limit the correlation length. As the quality of the raw data declines, the correlation length must be increased to insure valid correlations. An optimum correlation length for a good-quality dipmeter will be 2 to 4 in (5-10 cm). The search angle should be kept to the minimum necessary to identify the features, usually between 25° and 40°. Because the structural dip must be removed from these data prior to interpretation, the magnitude of structural dip to be removed must be added to this search angle. For instances where structural dip exceeds 20°, it is difficult to compute valid dips. This is because the

combination of very short correlation lengths necessary to resolve the dips and the 45° to 60° search angle will likely yield a lot of random dips. Although statistical methods can serve to eliminate most of these random computations, the reduced data set that remains will be smaller and less reliable as the search angle is increased.

The interpretation of this reduced and rotated dip data set depends on the identification of dip patterns that are commonly associated with local paleoslope and transport direction. These patterns are divided into two main groups (Campbell, 1968; Gilreath and Maricelli, 1964) which although separate, can have ambiguous interpretations.

In the case of a pattern caused by local paleoslope (or gravity), the pattern is described as having increasing dip magnitude with increasing depth with a relatively constant azimuth over a vertical interval, which is consistent with the expected thickness of the genetic units. This pattern is interpreted as resulting from slumping or draping.

Patterns associated with the transport direction are described as having decreasing dip magnitude with increasing depth with a relatively constant azimuth over a vertical interval, which is consistent with the expected thickness of the genetic units.

A "pattern" requires a minimum of two consecutive dips. The minimum difference that two dips must have before they can be considered as either increasing or decreasing in magnitude is usually considered to be 3° to 5°, with the lower dip magnitude usually being less than 5°. The azimuths should differ no more than 10° to 15°.

Before the interpreter starts looking for "patterns" that might identify the local paleoslope and transport direction, it is important to have some understanding of the more likely depositional environments (Gilreath and Stephens, 1971; Jageler and Matuszak, 1972). If the environment is identified, the interpreter may be able to effect an interpretation from either the local paleoslope direction or the transport direction alone. Or it may assist in allowing the interpreter to verify the directions rather than having to identify the directions with no information other than the dipmeter. Because most dipmeter interpretations have some ambiguities due to the limited data patterns compared with the numerous possible environments, it is always necessary to use a priority list to sort

75

through the possible interpretations and come down to the most likely interpretation. Any information that allows this list to be shortened will improve the final interpretation.

Because the directional information from the dipmeter is so critical to stratigraphic interpretation, it is prudent for the interpreter to examine the entire data set using azimuth frequency diagrams over 10 to 20 ft (3.0 to 6.1 m) intervals throughout the interval being interpreted. This will likely allow some azimuth patterns or concentrations to be identified. It is in these general azimuths that the interpreter should search for patterns. To attempt to identify patterns with no bias for azimuths may result in including extraneous data that cannot be included in an interpretation that must be extrapolated some distance from the well bore. The azimuth concentration(s) will usually be in one or two directions. If in two directions, they will commonly be at 90° or 180° orientation. Once these major azimuths are identified, it then remains to be determined whether they are associated with local paleoslope direction or transport direction. This becomes critical if no other information is available. Sedimentary deposits are usually perpendicular to the local paleoslope. If the local paleoslope azimuth can be identified, a valid offset well can be identified by moving on strike. But if only the transport direction can be determined, it becomes necessary to know the genesis or some other description of the sedimentary unit before the trend or strike of the reservoir unit can be determined.

It is usually necessary to examine a significant interval before an interpretation can be made. This requires a search for patterns above or below the reservoir. The depth interval chosen for this search must be depositionally coherent with the unit being described. This can often be determined by close examination of the dipmeter, other logs, or cores.

The structural and stratigraphic interpretations must be integrated into a single concept of the distribution of the reservoir. By understanding the depositional orientation and genesis of the reservoir as well as the structural orientation, a more complete picture of the reservoir from the dipmeter can be prepared for integration into the other descriptions available from cores, subsurface geology, and seismic and well control.

APPENDIX D. VELOCITY ANISOTROPY ON SAMPLES FROM THE VICKSBURG FORMATION SHELL A. A. MCALLEN B-18 WELL, (PREPARED BY WESTERN ATLAS INTERNATIONAL--CORE LABORATORIES, DECEMBER 1, 1989). (EXCERPT ONLY)

DISCUSSION

Compressional wave ultrasonic velocity has been measured across the diameter of core samples as a function of azimuth. The variations observed are interpreted in terms of microcrack opening in response to the stress removal after coring. If the horizontal stress in situ is directional in nature, the azimuth of maximum and minimum stress may be determined by the azimuth of velocity anisotropy measured on oriented whole core. The maximum velocity is normally interpreted to parallel the direction of least principle stress. The direction of minimum velocity corresponds to the direction of greatest principal stress. This is also the predicted azimuth for a vertical hydraulic fracture in this formation.

Of the ten samples from the Shell A. A. McAllen B-18 Well, sufficient anisotropy was measure on 7 (>2% anisotropy = Vmax/Vmin > 1.02). Interestingly though, even those with < 2% anisotropy had minimum and maximum velocities which correspond well with the others.

It appears that the measurements on the deepest sample, 13,447.5 - 13,448.0, results in ambiguous data, so the orientation was rechecked with the Bureau of Economic Geology. This sample appears to be in a slump zone throughout which they believe the orientation to be questionable. Also, this sample is a brittle shale which failed during an attempt to recheck velocity values. For these reasons, we recommend calculating average maximum and minimum values disregarding the data for this sample. This yields a maximum direction 176 degrees from true north and a minimum velocity of 87 degrees from true north. Thus, 87 degrees corresponds to the direction of greatest principle stress and also the predicted azimuth for a vertical hydraulic fracture.

REFERENCES

Ashford, T., 1972, Geoseismic History and Development of Rincon Field, South Texas: Geophysics, v. 37, p. 797- 812.

Berg, R. R., Shoemaker, P. W., and Marshall, W. D., 1979, Structural and Depositional History, McAllen Ranch Field, Hidalgo County, Texas: Gulf Coast Association of Geological Societies Transactions, v. 29, p. 24-28.

Campbell, R. L., 1968, Stratigraphic Applications of Dipmeter Data in Mid-Continent: American Association of Petroleum Geologist Bulletin, V. 52, p. 1700-1719.

Coleman, J. M., and Gagliano, S. M., 1964, Cyclic Sedimentation in the Mississippi River Deltaic Plain: Gulf Coast Association of Geological Societies, v. 14, p. 67-80.

Gardner, F. J., 1967, Typical Oil and Gas Fields of South Texas, Corpus Christi Geological Society, Corpus Christi, Texas, p. 221.

Gilreath, J. A., and Maricelli, J. J., 1964, Detailed Stratigraphic Control Through Dip Computations: American Association of Petroleum Geologist Bulletin, v. 48, no. 12, p. 1902-1910.

Gilreath, J. A., and Stephens, R. W., 1971, Distributary Front Deposits Interpreted From Dipmeter Patterns: Gulf Coast Association of Geological Societies Transactions, v. 21, p. 233-243.

Han, J. H., 1981, Genetic Stratigraphy and Associated Structures of the Vicksburg Formation, South Texas: The University of Texas at Austin, Ph.D. dissertation, p. 162.

Hill, D. P., Lennon, R. B., and Wright, C. L., 1991, Making an Old Gem Sparkle: The Rejuvenation of McAllen Ranch Field, Texas: Gulf Coast Association of Geological Societies, v. 41, p. 325-335.

Jageler, A. H., and Matuszak, D. R., 1972, Use of Well Logs and Dipmeters in Stratigraphic-Trap Exploration, in King, R. E., ed., Stratigraphic Oil and Gas Fields--Classification, Exploration Methods and Case Histories: American Association of Petroleum Geologist Memoir 16, p. 107-135.

Langford, R. P., Collins, G. E., Grigsby, J. D., Guevara E. W., Howard, W. E., Kocberber, J., Lord, M., Sippel, M., Wermund, E. G., 1991, Secondary Gas Recovery: Reservoir Heterogeneity and Potential for Reserve Growth Through Infield Drilling, an Example From McAllen Ranch Field, Hidalgo County, Texas. Topical Report, Gas Research Institute, Report in press, p. 282.

Langford, R. P., Grigsby, J. D., Howard, W. E., Hall, J. D., and Maguregui, J., 1990, Sedimentary Facies and Petrophysical Characteristics of Cores From the Lower Vicksburg Gas Reservoirs, McAllen Ranch field, Hidalgo County, Texas: Gulf Coast Association of Geological Societies Transactions, v. 40, p. 439-450.

Langford, R. P. and Lynch L. F., 1990, Diagenesis and Cement Fabric of Gas Reservoirs in the Oligocene Vicksburg Formation, McAllen Ranch Field, Hidalgo County, Texas: Gulf Coast Association of Geological Societies Transactions, v. 40, p. 451-458.

Marshall, W. D., 1978, Depositional Environment and Reservoir Characteristics of the Lower Vicksburg Sandstones, West McAllen Ranch Field, Hidalgo County, Texas: Texas A&M University, Master's thesis, p. 154.

Marshall, W. D., 1981, Turbidite Origin of the Oligocene Vicksburg Sandstone, McAllen Ranch Field, Hidalgo, County, Texas, *in* Recognition of Shallow-Water Versus Deep-Water Sedimentary Facies in Growth-Structure Affected Formations of the Gulf Coast Basin: Second Annual Research Conference, Gulf Coast Section, Society of Economic Paleontologists and Mineralogists.

Moran, J. H., Coufleau, M. A., Miller G. K., and Timmons, J. P., 1962, Automatic Computation of Dipmeter Logs Digitally Recorded on Magnetic Tapes: Journal of Petroleum Technology, v. 225, p. 771-782.

Picou, E. B., 1981, McAllen Ranch Field: Depositional Environments of Reservoir Sandstones and Associated Shales--The Shell Oil Company Perspective, *in* Recognition of Shallow-Water Versus Deep-Water Sedimentary Facies in Growth-Structure Affected Formations of the Gulf Coast Basin: Second Annual Research Conference, Gulf Coast Section, Society of Economic Paleontologists and Mineralogists.

Richards, G. L., 1986, Monte Christo Vicksburg Eckhart Field, Hidalgo County, Texas: Bulletin of the South Texas Geological Society, v. 26 no. 5, p. 27-44.

Ritch, H. J., and Kozik, H. G., 1971, Petrophysical Study of Overpressured Sandstone Reservoirs, Vicksburg Formation, McAllen Ranch Field, Hidalgo County, Texas: Society of Professional Well Log Analysts, 12th Annual Logging Symposium Transactions, preprint, p. 1-14.

Shoemaker, P. W., 1978, Depositional Environment and Reservoir Characteristics of the Lower Vicksburg Sandstones, East McAllen Ranch Field, Hidalgo County, Texas: Texas A&M University, Master's thesis, p. 128.

Straccia, J. R., 1981, Stratigraphy and Structure of the Rosita Gas Fields, Duval County, Texas: Gulf Coast Association of Geological Societies Transactions, v. 31, p. 191-200.